

UNIVERSITY OF OKLAHOMA

GRADUATE COLLEGE

SCALE UP REACTIVE FLOW IN HETEROGENEOUS POROUS MEDIA USING
CONTINUOUS TIME RANDOM WALK APPROACH

A THESIS

SUBMITTED TO THE GRADUATE FACULTY

in partial fulfillment of the requirements for the

Degree of

MASTER OF SCIENCE

By

KANG KANG
Norman, Oklahoma
2017

SCALE UP REACTIVE FLOW IN HETEROGENEOUS POROUS MEDIA USING
CONTINUOUS TIME RANDOM WALK APPROACH

A THESIS APPROVED FOR THE
MEWBOURNE SCHOOL OF PETROLEUM AND GEOLOGICAL ENGINEERING

BY

Dr. Maysam Pournik, Chair

Dr. Bor-Jier Shiau

Dr. Jeffrey H. Harwell

© Copyright by KANG KANG 2017
All Rights Reserved.

Dedication

To my dear mother, Peijun Wang for her love and support.

Acknowledgements

I would like to express my sincere gratitude to my supervising professor, Dr. Maysam Pournik, for his supervision and financial support throughout the duration of my graduate studies. Without the support and trust from him I would not have the chance to start my master program and complete it in one year at OU. Under his supervision I have learnt to think independently and innovatively, which I think will be very useful in my career ahead. I would also like to appreciate my committee members, Dr. Bor-Jier Shiau and Dr. Jeffery Harwell for their advices that help me a lot in my research.

I would also like to appreciate Dr. Elsayed R. Abdelfatah for his guidance and assistance in this thesis and related researches, and Yifu Han, Kailei Liu and Jiabo He for their comments on coding issues and contributions to ideas.

I owe a big thank you to all my friends who made my one-year graduate journey enjoyable and memorable. There are some people I know for a long time during my undergraduate years and some people who became my best friends in the last year. Even though I want to list all of them, I would specifically like to mention and appreciate friendship of Xu Yan, Haike Liang, Jingtong Lu, Keren Li, Na Yuan, Yi Jin, Bin Yuan, Da Zheng, Yu Jiang, Yunan Li, Akita, Ruben, Laura, Dennys, Daniel Backry, Scott Zickefoose, Hunter Bellavigna and John Xavier.

Finally, I would like to acknowledge my parents as their strong support and motivation to my graduate career. I am always encouraged by my mother's experience and personality to be a man of integrity, diligence and optimism.

Table of Contents

Acknowledgements	iv
List of Tables	vii
List of Figures.....	viii
Abstract.....	xi
Chapter 1 Introduction.....	1
1.1 Overview	1
1.1.1. Scale up reservoir properties	3
1.1.2. Scale up transport processes.....	4
1.1.3. Scale up reaction processes	6
1.2. Objective of research.....	7
1.3. Thesis Outline.....	8
Chapter 2 Modeling Non-Reactive Tracer Flow	10
2.1 Introduction	10
2.2 Mathematical Formulations of CTRW framework	12
2.3 Algorithm of particle tracking.....	16
2.4 Results and Discussions	19
2.4.1 Probability density of time increments.....	19
2.4.2 CTRW-PT simulation results	21
2.4.3 Sensitivity Analysis.....	30
2.5 Summary and Conclusions.....	32
Chapter 3 Modeling Reactive Nanofluid Flow	34
3.1 Introduction	34

3.2 Mathematical Model and CTRW Formulations	36
3.3 Modeling reactive processes.....	37
3.4 Results and Discussions	39
3.4.1 CTRW-PT simulation results	39
3.4.2 Sensitivity Analysis	42
3.5 Summary and Conclusions	44
Chapter 4 Scale Up Tracer and Nanofluid Flow	45
4.1 Introduction	45
4.2 Scale-up approaches	46
4.2.1 Scale up reservoir properties	46
4.2.2 Scale up transport using CTRW-PT approach	48
4.3 Results and Discussions	49
4.3.1 Scale up tracer flow in homogeneous system.....	49
4.3.2 Scale up nanofluid flow in heterogeneous system	51
4.3.3. Computational time of CTRW-PT and FDM approaches.....	53
4.4 Summary and Conclusions	54
Chapter 5 Conclusions and Future Work	55
5.1 Conclusions	55
5.2 Plans for future work.....	57
References	58

List of Tables

Table 2.1 — Parameters used and properties of tracer and porous media.	23
Table 3.1 — Parameters used in the experiments and simulations.	39
Table 4.1 — Recorded CPU time in seconds using CTRW-PT and Finite Difference Method in Python 2.7.0, with a grid size of 60 x 10.	54

List of Figures

Figure 1.1 — Recovery factor of reservoir fluids using various EOR methods at different volume scale (Lake et al. 2005, Leung 2009).....	1
Figure 2.1 — Illustration of difference between normal and anomalous transport, in terms of concentration profile along flow distance with time (Berkowitz and Scher 1998).....	11
Figure 2.2 — Schematic illustration of a) particle movement and locations in x-y coordinate and b) the gap between random temporal increments and time steps.	16
Figure 2.3 — Flowchart of tracking spatial location of a particle in x-y coordinate.	18
Figure 2.4 — Flowchart of tracking accumulated transition time of a particle.	18
Figure 2.5 — log-log plots of $\psi(t)$ with Peclet Number small to large from (a) to (d) with various β values for each case.	21
Figure 2.6 — Schematic of heterogeneous media prepared by Levy and Berkowitz (2003), where the black regions are packed with high-perm sands and white parts are packed with low-perm sands.	23
Figure 2.7 — Measured breakthrough curves fitted by ADE and CTRW-PT in homogeneous media. Flow rates and measured dispersion coefficients are (a) 36 ml/min, 0.037 cm ² /min, (b) 53 ml/min, 0.072 cm ² /min, and (c) 74 ml/min, 0.120 cm ² /min. Values of β are shown in each case.	26
Figure 2.8 — Measured breakthrough curves fitted by ADE and CTRW-PT in heterogeneous media. Flow rates and measured dispersion coefficients are (a) 35 ml/min, 0.212 cm ² /min, (b) 47 ml/min, 0.348 cm ² /min, and (c) 70 ml/min, 0.898 cm ² /min. Values of β are shown in each case.	27

Figure 2.9 — Concentration profiles of the case with injection rate of 36 ml/min in homogeneous system at time of (a) 50, (b) 100, (c) 200 and (d) 300 minutes.....	29
Figure 2.10 — Concentration profiles of the case with injection rate of 35 ml/min in heterogeneous system at time of (a) 50, (b) 200, (c) 400 and (d) 600 minutes.....	30
Figure 2.11 — Simulated breakthrough curves for tracer flow at injection rate of 36ml/min with various β and $t_2 = 5000 * t_1$	31
Figure 2.12 — Simulated breakthrough curves for tracer flow at injection rate of 36ml/min with various t_2 and $\beta = 1.71$	32
Figure 3.1— Fitted breakthrough curves for experiment a) low rate of deposition and b) high rate of deposition at the same injection rate of 1 ml/cm ³	40
Figure 3.2 — Concentration profiles of simulation of (a) experiment #33 with low rate of deposition and (b) experiment #45 with high rate of deposition at 200, 300,400 and 1100 minutes from top to bottom.....	41
Figure 3.3 — Fitted breakthrough curves for experiment (a) low injection rate of 1 ml/cm ³ (# 107) and (b) high injection rate of 10 ml/cm ³ (# 102) with similar rate of deposition.....	42
Figure 3.4 — Concentration profiles of simulation of (a) low injection rate of 1ml/cc (#107) and (b) high injection rate of 10 ml/cc (#102) at same PVI (Pore volume injected).....	42
Figure 3.5 — Simulated breakthrough curves for nanofluid flow experiment #45 at injection rate of 1ml/min and high rate of deposition with constant $t_2 = 5000 * t_1$	43
Figure 3.6 — Simulated breakthrough curves for tracer flow experiment #45 at injection rate of 1ml/min and high rate of deposition with constant $\beta = 1.7$	43

Figure 4.1 — Schematic of a reservoir property at two scales (Singh 2014).....	47
Figure 4.2 — Simulated breakthrough curves of tracer flow with injection rate of 74 ml/min, scaled up with 5 and 10 times.	50
Figure 4.3 — Concentration maps of tracer flow injected through one block at lab scale (a) and scaled up with 5 times (b) at time of 50, 100 and 200 minutes from top to bottom.....	50
Figure 4.4 — Relative permeability map at different spatial scales (a) lab scale, (b) scaled up for two times and (c) scaled up for four times.....	52
Figure 4.5 — Simulated breakthrough curves of nanofluid flow experiment#45 at injection rate of 1 ml/min and high rate of deposition, scaled up with 2 and 4 times....	52
Figure 4.6 — Concentration profiles of simulation of nanofluid flow experiment #45 injected through one block (a) at lab scale and (b) scaled up with 4 times at 200, 500 and 1500 minutes.....	53

Abstract

Reservoir heterogeneities strongly affect the fluid flow in porous media. The behavior of transport and reaction of fluid varies at different scales, leading to the discrepancies between laboratory experiments and field observations. The reactive processes in porous media may alter reservoir properties with different spatial and temporal scale, varying future transport and reaction behaviors. This thesis provides an efficient probabilistic approach to scale up coupled transport and reaction processes in heterogeneous porous media to field scale based on laboratory-scale information.

The continuous time random walk (CTRW) is a probabilistic framework which is always incorporating with particle tracking (PT) approach to model solute transport in heterogeneous porous medium. In CTRW-PT approach, the motion of solute particles is described as combination of random independent spatial and temporal increments in each walk step. The spatial and temporal increments, or normally called as transition distance and time, are chosen from a joint space-time probability density function by a stochastic process. The CTRW-PT approach simulates reactive fluid transport as non-reactive fluid. The modelling of reaction and dissolution is followed by in each time step, updating the change of porous medium and its effect on following transport and reaction.

The characteristic probability density function (pdf) is used to simulate the transport of fluid. Adjusting the ensemble parameter β and t_2 accounts for the effects of heterogeneity which leads to anomalous flow behavior: the fluid propagates along the “preferential” pathways with short transition times and “trapped” in some zones with long transition times. It mimics the macroscopic behavior that fluid has the tendency to propagate in

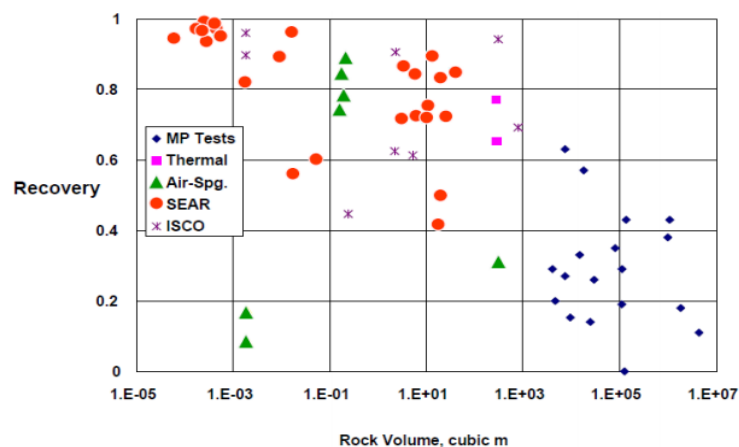
high-permeability zones and bypass the low-permeability zones. Simulations of non-reactive tracer flow and nanofluid flow under various conditions are performed at core-scale to obtain the key parameters in characteristic pdf by matching the experimental results. The effect of reactive process, heterogeneity and flow rate on flow behavior is analyzed. The CTRW-PT simulation captures the characters of anomalous behavior of delayed breakthrough. The model is run at larger scale as reservoir properties are scaled up properly. The core-scale simulation based on the characteristic pdf agrees with the experimental results. The large-scale simulation is implemented by using the characteristic pdf to describe flow behaviors in a large-scale domain. It is shown that CTRW-PT approach is more effective in large-scale modeling than solving advection-diffusion-reaction equation (ADRE) by finite difference method (FDM). The simulation results at large scale show that the flow response is spatial-dependent.

Compared to solving traditional ADRE, the utilization of CTRW-PT approach to model reactive fluid flow captures the characters of anomalous flow behavior, especially in highly heterogeneous porous media. By the probabilistic framework and stochastic process, this approach is more computational-efficient for scaling up lab-scale results to larger scale. It can consolidate the lab-scale understanding with field prediction to optimize the field treatment design.

Chapter 1 Introduction

1.1 Overview

The fluid flow in natural porous media involves both chemical and physical processes over different temporal and spatial scales. Most of the studies focus on verifying short-time and small-scale laboratory experimental results by numerical simulations. Numerous experiments and simulations have been done to discover the mechanisms of the advective-diffusive-reactive transport of solution in natural porous media to optimize the numerical model. The small-scale predictions at different conditions then can be obtained from the numerical model accurately. However, the discrepancies always exist between laboratory observations and field responses. The recovery factor of hydrocarbon decreases from core floods to field processes (Singh 2014). Figure 1.1 shows the how recovery factor decreases from small to large scale using various EOR methods such as surfactant flooding, thermal recovery and in-situ chemical oxidation. The optimum injection rate and minimum pore volume of matrix acidizing in carbonate increases from laboratory results to field treatment (Panga 2003).



The laboratory core floods yield accurate information of flow through porous media at core scale, but also exhibit variations from several tests. It means the information obtained from single core flood may not be enough representative at field scale. Therefore, the variation of responses of fluid flow in porous media at different spatial scales requires an appropriate scaling up approach to predict the large-scale processes based on small-scale results. Singh (2014) indicated that the functional relationship of transport process with spatial scales is the reason of the discrepancies of fluid flow responses from laboratory scale to field scale. The functional relationship can be represented by a numerical model which successfully matches the flow response at laboratory scale. It is then assumed that the flow processes at larger scale have the same behavior as it is at laboratory scale where the geological settings and operation conditions are consistent at all scales. The flow process at larger scale then is simulated as the model parameters are scaled up properly. To start the work of scaling up on fluid flow the conceptual understanding of it needs to be specified. The scaling up analysis contains two main concepts which are upscaling and scale up:

1. The upscaling which is the spatial scaling of physical properties, such as heterogeneities which introduce fluctuations across spatial scales. It is to substitute the heterogeneities variations in a geological model with fine grids with equivalent values and assign the values into coarse grids (Durlofsky 2003). For single phase flow, the effective permeability is always the interested grid property to be upscaled (Qi and Hesketh 2005, Salazar and Villa Piamo 2007). Permeability is intrinsic by nature and simple volumetric arithmetic averaging method is no longer valid.

2. The scaling up which is a numerical process to represent the observed flow behavior at smaller scale to a larger scale. Unlike upscaling, the scaling up does not assume a consistent flow conditions like flow rate across different scales. A typical example of scaling up is to predict the recovery factor at field scale with the known responses from core flood experiments in the laboratory. The challenge of scaling up is always considered as the different flow responses induced by scale-dependence heterogeneity variations across different scales (Singh 2014). Berkowitz and Scher (1998) used a probabilistic approach to scale up the contaminant transport temporally and spatially, where they indicated that the heterogeneity affects the transport process significantly by introducing non-Fickian (anomalous) diffusion.

This work focuses on scaling up fluid transport and reaction processes and the reservoir properties at larger scale is simulated from the information obtained from laboratory.

1.1.1. Scale up reservoir properties

One of the assumptions of scaling up is the consistent reservoir properties which include rock composition, porosity and permeability. It is assumed that all the reservoir properties at small scale have been obtained from core samples. Then the properties are properly scaled up by a consistent covariance model to a larger scale with finer scale. Finally, the properties are arithmetically or harmonically averaged to yield a coarse grid model at larger scale.

1.1.2. Scale up transport processes

The flow process is spatial scale-dependent due to the variations of heterogeneities and boundary conditions across scales. Also, the reactive fluid flow through porous media associated with chemical reactions change reservoir properties with time. Therefore, the transport and reaction process are functions of changing reservoir properties which vary with time as well as space. The scale up approach needs to take care of both spatial and temporal variations on the transport and reaction processes to accurately predict the flow behavior. The popular approaches to scale up fluid flow are dimensionless groups, ensemble or volumetric averaging transport equations from fine to large scale and particle tracking approaches. Dimensionless groups are dimensionless parameters scaled using Shook's dimensionless groups by flow related variables such as effective aspect ratio of permeability, mobility ratio, domain dimensions, flow rate etc. (Shook et al. 1992). The dimensionless groups can define the flow processes and to test if the flow has similar response assuming the groups are equal across scales (Li et al. 1996). The averaging transport equations can provide equivalent transport parameters as a function of scale by applying ensemble or volume averaging formalisms (Dongxiao and Winter 1999, Whitaker 2013). The particle tracking approach is to simulate flow as random particles being injected into the porous media and transport through it. The transport of particles is simulated by statistical process and partial physics. Two main approaches of particle tracking are 1) Random walk particle tracking (RWPT), and 2) Continuous time random walk (CTRW).

The random walk particle tracking makes the particles move under a combination of convective and dispersive effects. The convective effect is solved by defining an

instantaneous flow velocity of particle. The dispersive effect is explained by a Brownian motion which mimics the random process of dispersion. A classic equation of RWPT which describes the movement of a particle (Kitanidis 1994):

$$s(t + dt) = s(t) + \vec{u}(s(t))dt + (2D(s(t))dt)^{\frac{1}{2}}\xi \quad (1.1)$$

where,

s is spatial location of particle, can be in x, y and z direction in a 3-D domain

t is time

dt is time step

\vec{u} is velocity vector

D is dispersion coefficient

ξ is independent normally distributed variable with zero mean and unit variance.

The continuous time random walk is a probabilistic framework introduced by Montroll and Weiss (1965) which describes the movement of particle that is controlled by Monte-Carlo sampling following a specific transition probability distribution. The transition probability density function (pdf) of the distribution obeys the physics of fluid flow and properties of porous media. The CTRW simulates the movement of particles by assigning independent random temporal and spatial increments to current location of each particle. The random temporal and spatial increments follow the joint space-time transition probability distribution. A typical form of the joint space-time pdf for non-reactive fluid flow is (Edery et al. 2010):

$$\vec{s}^{i+1} = \vec{s}^i + \vec{\zeta}^i, \quad t^{i+1} = t^i + \tau^i \quad (1.2)$$

$$\vec{u}^i = \frac{\vec{s}^i}{\tau^i} \quad (1.3)$$

where,

s^i, t^i denotes the spatial and temporal location of particle at i th step of transitions, or walks.

ζ^i and τ^i are random temporal and spatial increments assigned to a particle at i th step,

\bar{u}^i is the velocity of particle which can be derived by dividing the spatial increment with the temporal increment at i th step.

CTRW-PT is efficient to simulate and scale-up fluid flow in a heterogeneous porous media due to it can well quantify non-Fickian (anomalous) behavior. The additional advantages of CTRW include that it can be applied in a grid-free system and it is computational efficient compared to finite difference method (McCarthy 1993). However, the limitation of CTRW is that the simulation process does not capture full physics of transport in the formalism. Instead, it uses a probabilistic framework to match the laboratory observations and assume the particles move in a similar way at both small and large scales. Though the formalism of CTRW does not incorporate full physics, it satisfies the conditions and requirements of this work.

1.1.3. Scale up reaction processes

Reactive flow such as nanoparticles transport involves interaction between the transported species and the porous medium (Abdelfatah et al. 2017a, Abdelfatah et al. 2017b, Abdelfatah et al. 2014, Abdelfatah et al. 2017c, Abdelfatah et al. 2017d). The reactions occurred during the flow process is simulated separately from transport at the end of each time step. The reaction rate is calculated based on the condition of reservoir

and fluid properties at that time step. It is notable that the change in reservoir and fluid properties will affect the transport and reaction in the following time step.

1.2. Objective of research

The heterogeneities cause the fluid transport through porous media to vary at different scales. The reactions during the transport process changes the reservoir properties and induces following evolutions with time and space. The probabilistic formulism of CTRW can handle the non-Fickian diffusion induced by the scale-dependent heterogeneity. The primary objective is to provide an efficient approach to predict flow response at larger scale based on the response obtained from laboratory experiments. The approach should scale the spatial and temporal parameters accounting for chemical reactions in heterogeneous porous media.

The CTRW framework incorporating particle tracking (PT) approach is applied to simulate and scale up the reactive flow process. The objective is processing following three steps:

1. Use CTRW formulism to generate the characteristic transition pdf which capture the behaviors of transport at laboratory scale by matching the core flood results. The chemical reactions are modeled separately at each time step which alter the reservoir properties. The key parameters of the characteristic transition pdf vary as operation conditions such as injection concentration and flow rate change. The generate pdf represents the ensemble behavior and response of the reactive flow in porous media.

2. Scale up the reservoir properties which keeps consistent covariance as they are at small scale. The domain is also scaled up to greater length scales which are close to field conditions with finer grid blocks. The operation parameters like injection rate is directly increases depending on the ratio of field domain volume to core volume.
3. By assuming the transport and reaction processes behaves in a similar way from small to large scales, the CTRW formulism is used to scale up the fluid transport. Using the same parameters for flow behavior and porous media with scaled flow rate, the temporal and spatial increments are scaled. The CTRW-PT model then is run at larger scale to predict the response at field scale.

1.3. Thesis Outline

Chapter 2 discusses the concepts and formulism of CTRW framework. The characteristic transition pdfs which yield characteristic probability distribution of spatial and temporal increments are generated for several case studies. The particle tracking algorithm to normalize the temporal and spatial movements of particles is presented. A non-reactive (tracer) flow in homogeneous and heterogeneous media is simulated by CTRW-PT approach by historical matching the experiment results. Sensitivity analysis is performed to investigate the effect of injection rate, injection concentration and heterogeneity. Chapter 3 presents the study of a reactive (nanofluid) flow in homogeneous and heterogeneous media with chemical reactions of nanoparticle deposition on rock pore surface occur. The same model of CTRW-PT is run to simulate the transport with the chemical alternations accounted. Chapter 4 demonstrates the scale-up of reservoir properties, the size of domain and the characteristic transition pdf. The simulations at

larger length scale and finer grid are run to investigate the effect of spatial scales and heterogeneity. The advantage of CTRW-PT approach over solving ADRE with finite difference method (FDM) is presented. Chapter 5 summarizes key findings of the research and the plan of future works.

Chapter 2 Modeling Non-Reactive Tracer Flow

2.1 Introduction

Fluid flow in porous media is always studied as a superposition of advection, diffusion and reaction processes. The most popular method used to model fluid flow is the numerical simulation using the advection-diffusion-reaction equation (LaBolle et al. 1998). For tracer transport, the source/sink term accounting for reactive process is neglected and the equation is reduced to advection-diffusion equation (Mostofizadeh and Economides). The idea of this method is to resolve the flow velocities in each fine grid block of a domain to construct a concentration map with time by ADRE numerically. The critical assumption of ADRE is the ensemble solutions of all small-scale blocks can capture larger-scale behaviors. However, in some cases, the solutions of ADE fail to capture the macroscopic behavior of the transport in heterogeneous or even homogeneous media. This phenomenon is observed from lab (Silliman and Simpson 1987) to field scale (Boggs et al. 1992), and evidently because the heterogeneities present at all scales and need be counted (Berkowitz and Scher 1998). This so-called non-Fickian or anomalous transport where the diffusion has a non-linear relationship to time. The anomalous diffusion is defined as:

$$\langle MSD^2 \rangle \propto t^\alpha \quad (2.1)$$

where,

MSD is the mean square displacement of a particle.

α is a constant to evaluate the diffusion type. For a normal or Fickian diffusion $\alpha=1$.

Otherwise, the non-Fickian, or anomalous diffusion occurs.

The anomalous diffusion is observed to have different behaviors of fluid flow than normal diffusion (Figure 2.1). The concentration profile along flow direction is always characterized by a slowly advancing maximum concentration and a rapidly advancing front, resulting in the late arriving of majority of fluid (Rhodes et al. 2009). Vlahos et al. (2008) conducted experiments with particles in fluid, and explained anomalous transport as some of particles are ‘trapped’ in some locations in porous media, where particles stay for ‘unusually’ long times in a relatively small spatial area. It is explained that the particles tend to avoid slow-flowing zones and will spend more time to find a fast-flowing pathway to propagate. For solution transport in heterogeneous medium, the fastest path between two points may not be a straight line. The existence of preferential pathways leads to early-time arrivals or late-time delays (Berkowitz and Adler 2015). Recently, the CTRW framework has been proved as an efficient approach to provide general and effective mean to quantify anomalous transport (Berkowitz and Scher 1998).

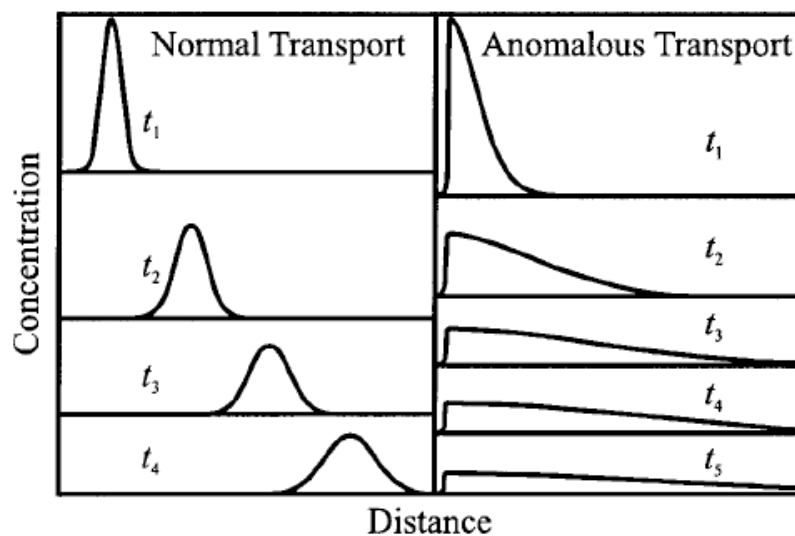


Figure 2.1 — Illustration of difference between normal and anomalous transport, in terms of concentration profile along flow distance with time (Berkowitz and Scher 1998).

2.2 Mathematical Formulations of CTRW framework

Non-reactive tracer flow only accounts for advective and diffusive displacement so that the ADRE reduces to advection-diffusion equation (Mostofizadeh and Economides) for non-reactive tracer flow. CTRW treat the solution in porous media as particles and the motion of particles undergo independent spatial and temporal transitions. The transitions can be explained by random walks spatially and temporally which contributed by the combined advective and diffusive processes. Berkowitz and Scher (1998) derived the CTRW transport equation in the special case of normal diffusion and illustrated that it has equivalent form of an ADE as a result of the ensemble average. As discussed in Section 1.1.2, the particle movement is governed by equations of motion (1.2) and (1.3). The increments ζ^i and τ^i follow the spatial and temporal transition probability distributions and are chosen from the joint transition probability density function $\psi(\vec{s}, t)$ which reflects the reservoir properties such as pressure and pore structure heterogeneity.

The joint space-time particle transition probability density function can be written in a decoupled form (Edery et al. 2010):

$$\psi(\vec{s}, t) = F(\vec{s})\psi(t) \quad (2.2)$$

where,

$F(\vec{s})$ is the pdf of spatial increments.

$\psi(t)$ is the pdf of temporal increments.

The functional form of the pdf is critical because they govern the behavior of anomalous transport. Edery et al. (2010) provides the equations of pdfs employing a truncated power law (TPL) to capture the anomalous behavior:

$$pdf \text{ for space: } F(\vec{s})d\vec{s} = sp(s)ds\Omega(\phi)d\phi \quad (2.3)$$

$$p(s) = \lambda_s^2 \exp(-\lambda_s s) \quad (2.4)$$

$$\Omega(\phi) = \mathcal{N}[0, \sigma] \quad (2.5)$$

$$pdf \text{ of time: } \psi(t) = \lambda_t \exp(-\lambda_t t), \quad \text{Normal} \quad (2.6)$$

$$\psi(t) = C \frac{\exp\left(-\frac{t}{t_2}\right)}{\left(1 + \frac{t}{t_1}\right)^{1+\beta}}, \quad \text{Anomalous} \quad (2.7)$$

where,

$p(s)$ is the pdf of transition distance along the flow direction.

$\Omega(\phi)$ is the pdf of angular vector for transition distance.

$\psi(t)$ is the pdf of transition time which follows exponential distribution for normal transport and a combined exponential-TPL distribution for anomalous transport.

t_1 is the characteristic advection time.

t_2 is the cut-off time to normal transport, or characteristic diffusion time.

β is the power law exponent.

λ_s , λ_t and C are normalization coefficients.

The angular vector accounts directions of particle movement in a 2-D space. It follows a normal distribution with standard deviation of σ , assumed to be $\frac{\pi}{4}$. Increasing standard deviation increases the degree of transverse dispersion in the CTRW-PT simulation (Dentz et al. 2008). In heterogeneous media, the angular vector of a particle is assumed

to be controlled by permeability in neighbor grid blocks. A ratio of permeability in neighbor grid block $\frac{k(i,j-1)}{k(i,j+1)}$ is added into the model to determine which direction a particle is most likely to advance through a stochastic process. For example, $\frac{k(i,j-1)}{k(i,j+1)} < 1$, which means the block $(i,j+1)$ has higher permeability, resulting in more possibility of the particle to have a vector angle greater than 0 to have a tendency of transverse direction to block $(i,j+1)$. It reflects the fact that fluid tends to flow through high-perm zone instead of low-perm zone. β represents the effect of heterogeneity on the transport behavior. As $\beta \geq 2$ the transport becomes normal, and more heterogeneous system yields a smaller value of β . λ_s , λ_t and C are normalization coefficients to make the integral of pdfs $p(s)$ and $\psi(t)$ equal to 1, noted that λ_s^2 is used because a 2-D domain is studied.

For modeling anomalous transport, equations 2.1 through 2.5 and 2.7 are used. We need to generate pdfs $F(\vec{s})$ and $\psi(t)$ appropriately to start CTRW-PT simulation. The treatments of transport parameters are explained below:

1. t_2 can be approximately calculated by $\frac{\bar{s}^2}{4D_m}$, where \bar{s} is the average transition distance and D_m is the molecular diffusion coefficient. It reflects the longest time a particle will take to diffuse a transition distance. While Berkowitz et al. (2006) suggests that it can be roughly taken as 1000 to 10000 times of t_1 from their experimental observations.
2. λ_s and t_1 are parameters which need to be solved through some calculations based on experimental results from laboratory. The mean particle velocity, u_ψ , and the

generalized particle dispersion coefficient, D_ψ , are defined as the first and second spatial moments of $\frac{p(s)}{t}$, respectively.

$$u_\psi = \frac{\bar{s}_x}{\bar{t}} = \frac{\int_0^\infty p(s)s^2 ds \int_0^\pi \Omega(\phi) \cos(\phi) d\phi}{\int_0^\infty \psi(t)t dt} \quad (2.8a)$$

$$D_\psi = \frac{\bar{s}_x^2}{\bar{t}} = \frac{\int_0^\infty p(s)s^3 ds \int_0^\pi \Omega(\phi) \cos^2(\phi) d\phi}{\int_0^\infty \psi(t)t dt} \quad (2.8b)$$

where,

\bar{s}_x is the mean transition distance and \bar{t} is the mean transition time.

Inserting equations 2.4, 2.5 and 2.7 into 2.8a and 2.8b yields:

$$u_\psi = \frac{2\exp(-0.5\sigma^2)}{\lambda_s t_1} \quad (2.9a)$$

$$D_\psi = \frac{1.5 + 1.5\exp(-2\sigma^2)}{\lambda_s^2 t_1} \quad (2.9b)$$

where,

u_ψ and D_ψ can be estimated from experimental results like breakthrough curves. Then the transport parameters λ_s and t_1 in $\psi(\vec{s}, t)$ can be solved by equations 2.9a and 2.9b.

3. β is the key parameter in CRTW formulism which controls the behaviors of plume in simulation. β is to be adjusted to historical match the simulated breakthrough curve to the one obtained from core flood.
4. As the simulation results are well matched with experimental results the characteristic pdf $\psi(\vec{s}, t)$ is derived by the fitted parameters β and t_2 . The spatial distributions of tracer concentration in 2-D domain are recorded to demonstrate the behavior of anomalous flow in heterogeneous porous media with time. The concentration profiles

demonstrate the effect of heterogeneity, injection rate and reactive process on dispersion, which are described by β and t_2 .

2.3 Algorithm of particle tracking

The CTRW modeling defines the motion of particles by assigning each particle a random spatial and temporal increment at each time step (Berkowitz et al. 2006). The particles injected into the porous media undergo spatial and temporal random ‘walks’, or transitions. In simulation, particle tracking is to monitor and record locations of particles inside the domain at the end of each time step. Spatial locations of particle are calculated and recorded by adding the random spatial increments and angular vector into its previous location in x-y coordinates (Figure 2.2a). The time spent is accumulated by simple summation of time increments at each transition. The transitions be approximately treated as pore-to-pore movements, where Darcy’s law is valid (Rhodes et al. 2009). However, there exists difficulty to track the particles at the end of each time step because each particle is assigned with different temporal increments chosen from stochastic processes. The difference between temporal increments τ^i and time step dt leads to the gap of particle tracking at same time (Figure 2.2b).

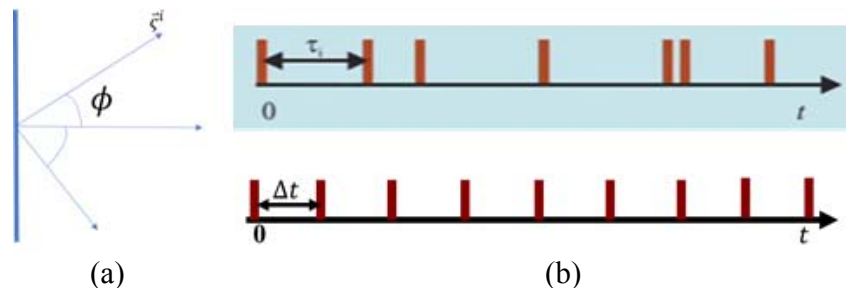


Figure 2.2 — Schematic illustration of a) particle movement and locations in x-y coordinate and b) the gap between random temporal increments and time steps.

According to (Edery et al. 2011), a ‘midflight technique’ is employed to normalize the timeline to make the particle tracking at the end of each time step possible. This technique is to freeze a particle in mid-flight (during a transition) at the end of a time step while calculating the current location and transition time it spent. The tracking of current location and transition time are achieved by the particle velocity of current flight. Recall equation 1.3, the velocity of a particle during i th transition is determined. Once a particle is injected into the domain, its spatial and temporal transitions are recorded until each time step is reached. At the end of each dt , all the particles in the domain are frozen in midflight. If a particle completed its previous flight before a time step dt , new spatial and temporal increments are assigned to the particle and the particle can advance by the time was left from the dt with new velocity during the current flight. If a particle has an accumulated transition time greater than the total simulation time until current dt , the accumulated spatial location and transition time of this particle is reduced by whatever time excess from the total simulation time. The particle continues to move with the velocity during the uncompleted flight as simulation of next time step begins. This technique allows the particle motion to be tracked at the normalized time steps to avoid any bias that may introduced by the gap between temporal increments and dt . The flowcharts of tracking the location and transition time of a particle are shown in Figure 2.3 and 2.4. The initial and boundary conditions are set to be:

$$\begin{aligned} C(x, y, t = 0) &= 0, \\ C(0, y, t) &= C_{inj}, \\ \frac{\partial C(L, W, t)}{\partial x} &= 0 \end{aligned} \tag{2.10}$$

where,

x, y are the distance in longitudinal and transverse direction.

L, W are the length and width of the 2-D domain.

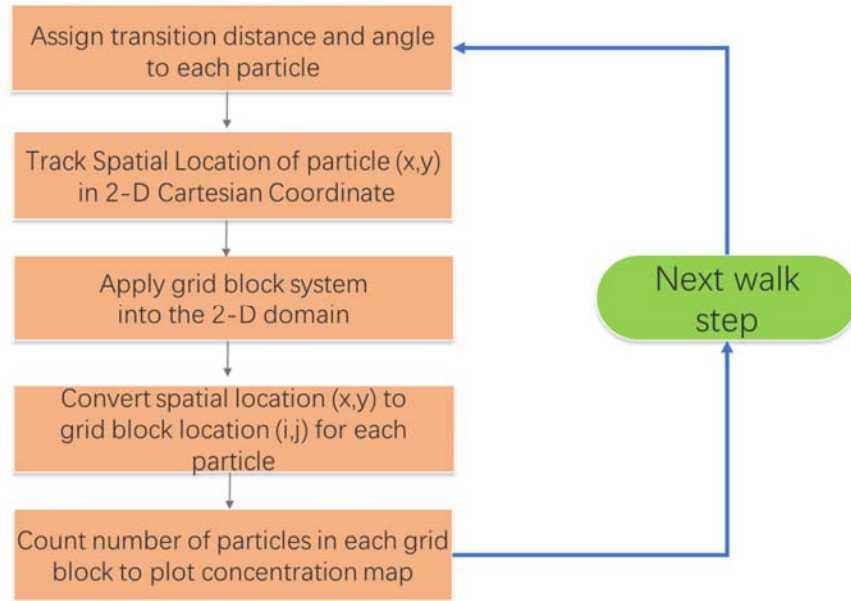


Figure 2.3 — Flowchart of tracking spatial location of a particle in x-y coordinate.

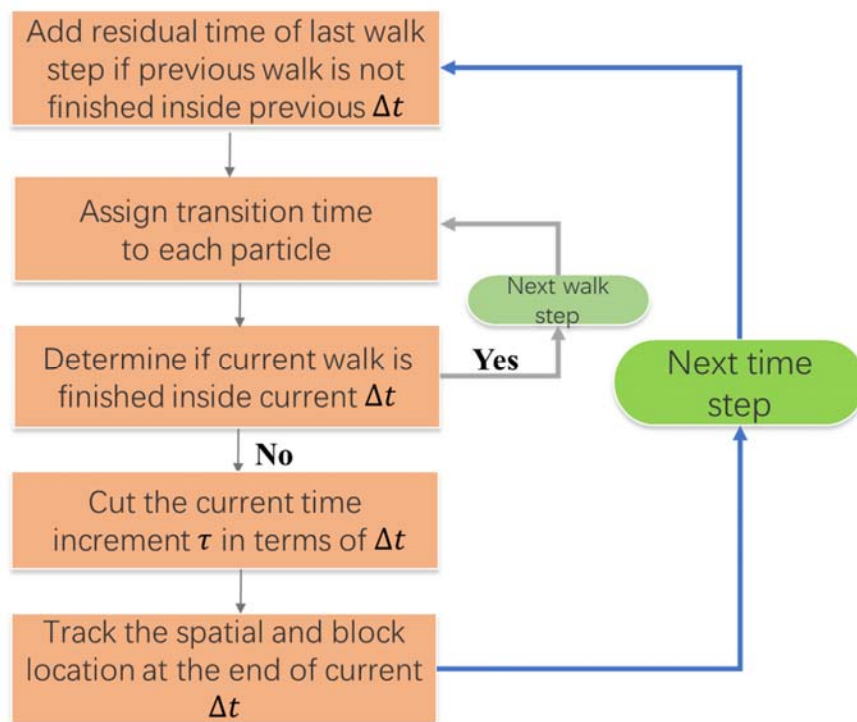


Figure 2.4 — Flowchart of tracking accumulated transition time of a particle.

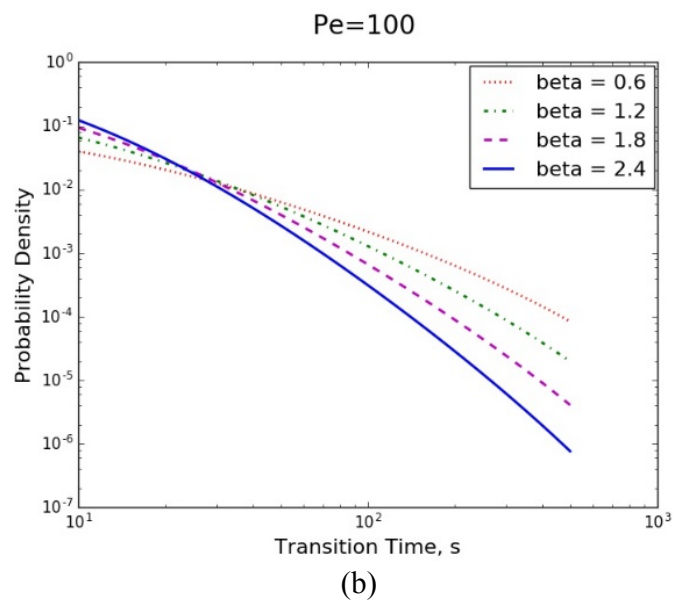
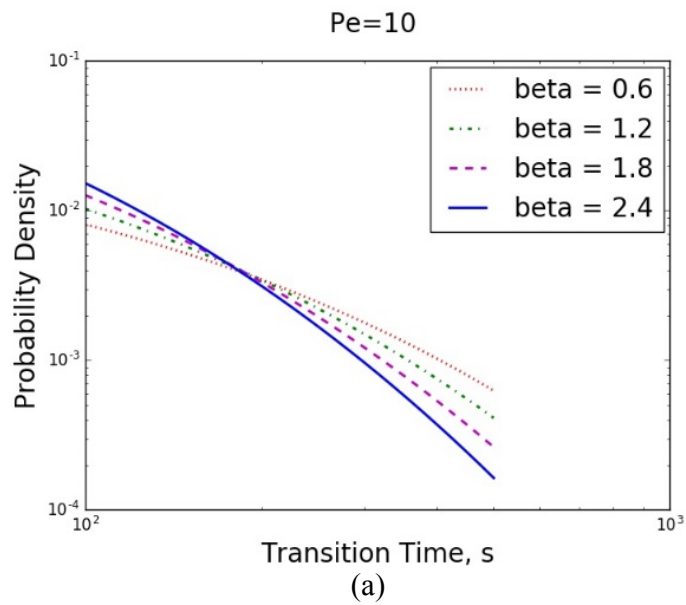
2.4 Results and Discussions

2.4.1 Probability density of time increments

The temporal and spatial increments assigned to particles are chosen randomly from characteristic probability distributions which are considered as a stochastic process. Like any stochastic process, the joint time-space pdf $\psi(\vec{s}, t)$ can produce an ensemble average of all possible transitions to approximate flow behavior. For $\psi(\vec{s})$, the transition distance increments are mainly determined by mean flow velocity and dispersion coefficient which can be obtained from laboratory experiments. For $\psi(t)$, The transition time increments are controlled by the parameters of β and t_2 . The key parameter β and t_2 in $\psi(t)$ describes the nature of transport fundamentally by controlling the time probability function $\psi(t)$. Smaller β and greater t_2 means a more heterogeneous media, higher level of anomalous transport which are brought by higher longitudinal and transverse dispersion.

The probability density of $\psi(t)$ are plotted to compare the effect of Peclet Number and adjusted β values (Figure 2.5). The mean transition distance is assumed to be constant in four tests with no changes of porous media involved. t_2 is then set to be a constant by the way it is defined ($\frac{\bar{s}^2}{4D_m}$). The Peclet Number is defined as $\frac{u\psi\bar{s}}{D_m}$, which can be interpreted as the ratio of advective transport rate to diffusive transport rate. As Peclet number increases, shorter transition time increments have higher probability to present due to higher advection to diffusion rate. At the same Peclet number, increasing β makes the curve of probability rotate clockwise with a fixed center point. It shows higher probability of short time increments and less probability of long time increments. From the view of

particle tracking method, higher β value means more particles move with advection-dependent velocity and less particles move with diffusion-dependent velocity. In a word, high β represents less anomalous diffusion and more convergence to normal transport. In CTRW-PT simulation, β is the key parameter to show the effect of microscopic heterogeneity on macroscopic flow behavior.



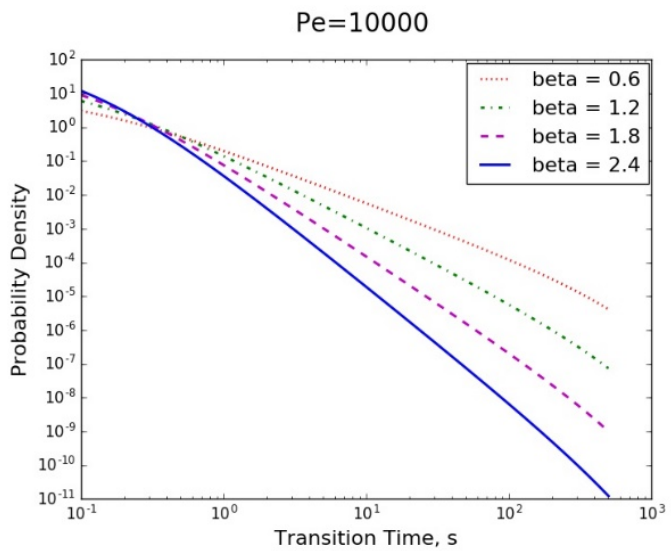
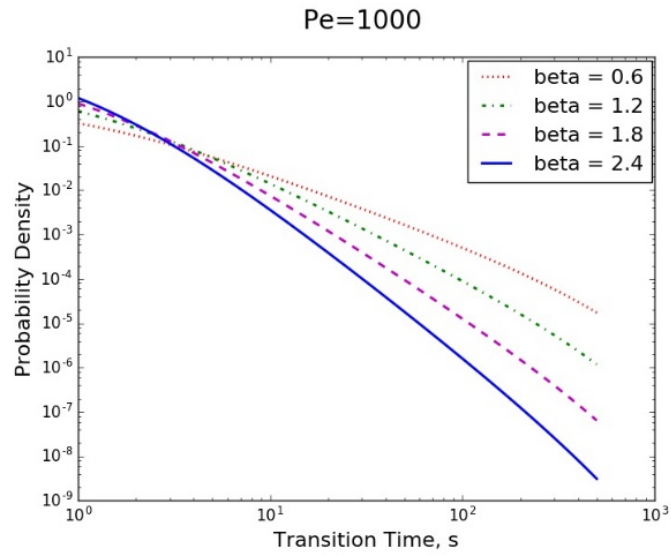


Figure 2.5 — log-log plots of $\psi(t)$ with Peclet Number small to large from (a) to (d) with various β values for each case.

2.4.2 CTRW-PT simulation results

Six laboratory experiments done by Levy and Berkowitz (2003) of tracer (NaCl) flowing through homogeneous and heterogeneous sand pack at low to high injection rate are simulated and matched by CTRW-PT approach with β . The parameters used in the

simulation keep the same as the experiments (Table 2.1). There are three experiments conducted in homogeneous sand pack and another three in heterogeneous sand pack. The same sand is used in homogeneous system and two kinds of sands are packed together in heterogeneous system. The packed pattern of sand in randomly packed heterogeneous system is illustrated in Figure 2.6. The heterogeneous system reproduces Silliman and Simpson's (1987) 'uniform heterogeneous' structure to better capture the late breakthrough time and tail of tracer plume which are the ensemble result of anomalous transport. The CTRW-PT simulations are run to fit the breakthrough curves by adjusting value of β . The grid blocks in heterogeneous case is made based on the packing patterns of Sand I and Sand II. The size of each block in heterogeneous case is the size of every low-perm sand packed in the media.

The simulation results with ADE fittings given by Levy and Berkowitz (2003) are shown in Figure 2.7 and 2.8. The ADE assumes a piston-like displacement, that the direction and magnitude of flow velocity is the same as injection velocity:

$$\frac{\partial(\phi C)}{\partial t} + u \frac{\partial C}{\partial x} = D\phi \frac{\partial^2 C}{\partial x^2} \quad (2.11)$$

The CTRW-PT fittings match the experimental breakthrough curves well, while the ADE fittings deviate from the experimental results at different levels. Figure 2.9 and 2.10 show 2-D concentration profiles of homogeneous case (a) and heterogeneous case (a) as time proceeds. Though the grid block sizes in two systems are different, the domain sizes are the same, and the concentration profiles are adjusted to the same size to be consistent with their true domain size.

Table 2.1 — Parameters used and properties of tracer and porous media.

Domain length, cm	86
Domain width, cm	45
Domain height, cm	10
Number of blocks in homogeneous case	17x9
Number of blocks in heterogeneous case	28x30
Initial porosity	0.3
Sand I permeability, m ²	5·10 ⁻⁹
Sand II permeability, m ²	1.5·10 ⁻¹⁰
Molecular diffusion Coefficient, cm ² /s	1·10 ⁻⁵
Injection concentration, M	0.5

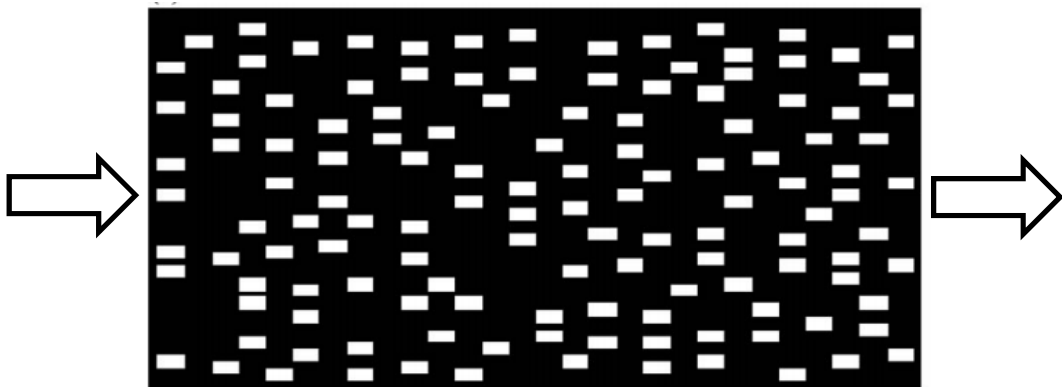


Figure 2.6 — Schematic of heterogeneous media prepared by Levy and Berkowitz (2003), where the black regions are packed with high-perm sands and white parts are packed with low-perm sands.

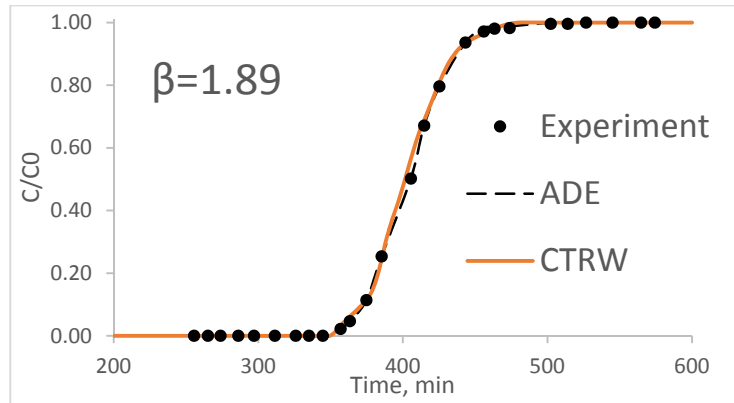
As discussed in Section 2.2.1, the mean velocity is obtained at dimensionless concentration (C/C_0) reaches 0.5. Therefore, the central region of breakthrough curves is the basis for both of CTRW and ADE simulation. This explains that all six fittings using those two approaches have good convergence near the central region of breakthrough curves. However, at early and late time of breakthrough process, ADE fittings show more

breakthrough at early and late time, respectively. The CTRW-PT fittings better capture the late breakthrough before and after the central region which distinguish the normal and anomalous transport. The comparisons show the different between normal and anomalous transport, which are properly described ADE and CTRW approaches, respectively. The difference is in anomalous transport the front of plume delays the breakthrough in early time and the long tail of plume also delays breakthrough in late time, which is captured by β in CTRW. While in normal transport, the plume shows a Gaussian shape without delaying the breakthrough. In CTRW, the parameter β characters the feature of anomalous transport and the value of it indicates the level of deviation of anomalous transport to the normal transport.

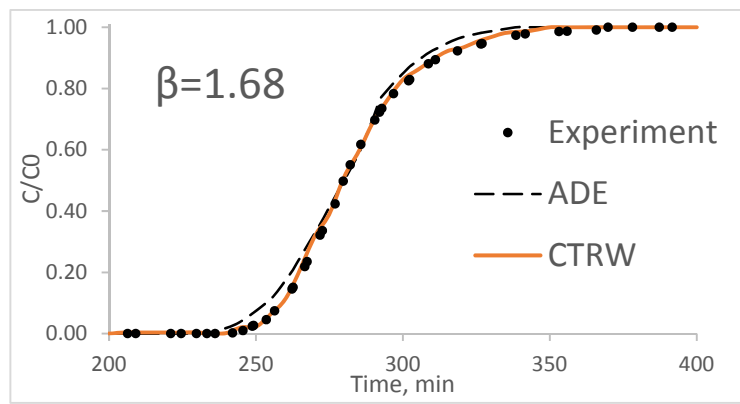
Figure 2.7 show the fittings of breakthrough curves by ADE and CTRW-PT in homogeneous media at different injection rate and measured dispersion coefficient. Figure 2.8 show the cases in heterogeneous media. The three cases in the same porous media are compared to investigate the effect of injection rate. Each case with similar injection rate in homogeneous and heterogeneous systems are also compared to investigate the effect of heterogeneity. These two effects are finally represented by β and t_2 , where t_2 is calculated by $(\frac{s^2}{4D_m})$. The adjusted β values are labelled in each figure.

Comparing the two (a), (b) and (c) figures in two systems, β in homogeneous cases is greater than it is in heterogeneous cases at similar injection rate, indicating that heterogeneity makes transport more anomalous. In addition, the breakthrough is earlier in homogeneous than heterogeneous system with greater β value at low flow rate. It reveals the effect of anomalous diffusion on plume shape which delays the breakthrough. Figure 2.7(a) and 2.8(a) show the breakthrough curves of two experiments at similar

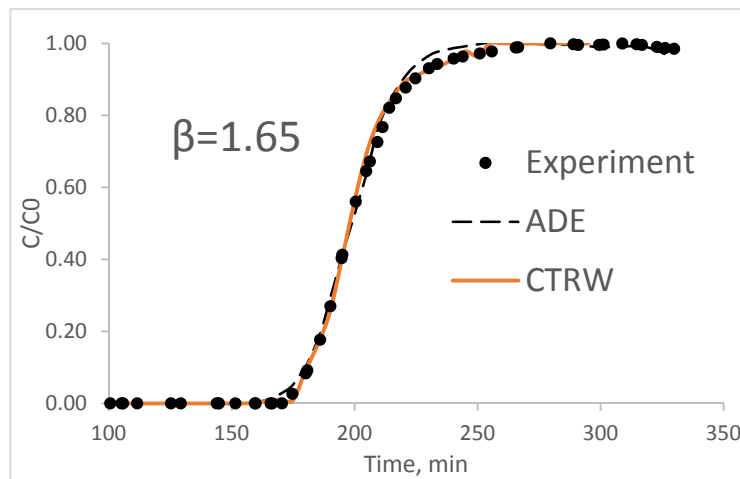
injection rate in homogeneous and heterogeneous system, with a much larger dispersion coefficient in later one. There exists a difference about 1500 minutes between homogeneous and heterogeneous cases as the effluent relative concentration becomes unity. The reason might be the significant 'trapping' effect on fluid brought by the heterogeneity at pore scale (Berkowitz et al. 2006). Figure 2.7(c) and 2.8(c) show the breakthrough in heterogeneous system is earlier than it is in homogeneous system at high injection rate, with a smaller β . However, the late time breakthrough, which is when the effluent relative concentration becoming unity, is later in heterogeneous system than it is in homogeneous system. The front that tries to find its fastest pathway flows ahead and breakthrough occurs at very early time, leaving the majority of fluid to struggle in slower flow regions (Levy and Berkowitz 2003). This explains that the breakthrough time of effluent concentration reaching unity decreases with smaller β . The time in homogeneous case (c), 250 minutes, is smaller than it is in heterogeneous case (c), which is 400 minutes. The fluid flushes uniformly through the whole media in homogeneous case so the complete flush is achieved early. However, in heterogeneous system, only a small portion of fluid flow through the fast paths and most of the fluid undergoes anomalous transport, spending more time in the slow paths before the arrival to effluent point. As an overall description of flow, smaller β means more deviation from normal transport and anomalous transport becomes more important.



(a)

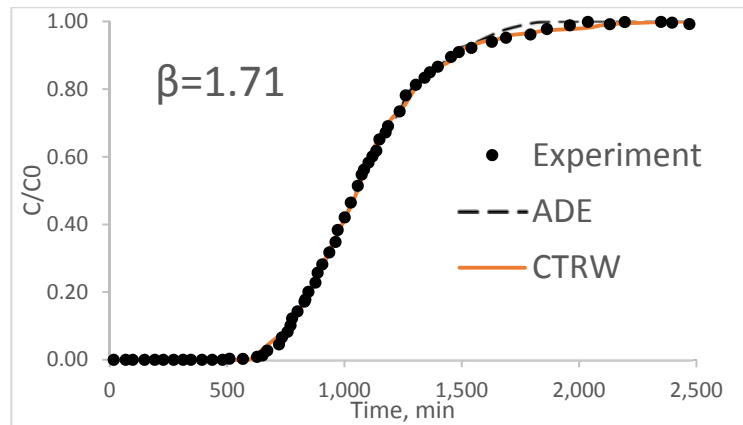


(b)

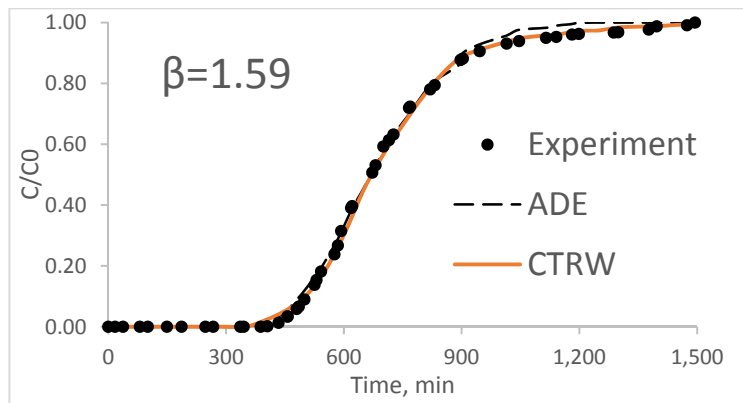


(c)

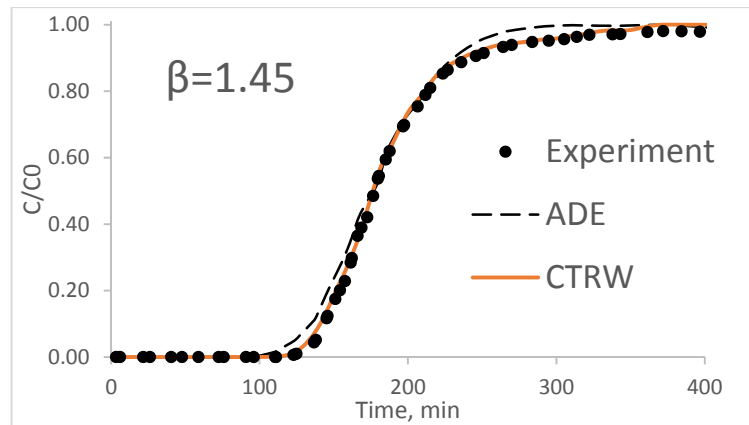
Figure 2.7 — Measured breakthrough curves fitted by ADE and CTRW-PT in homogeneous media. Flow rates and measured dispersion coefficients are (a) 36 ml/min, 0.037 cm²/min, (b) 53 ml/min, 0.072 cm²/min, and (c) 74 ml/min, 0.120 cm²/min. Values of β are shown in each case.



(a)



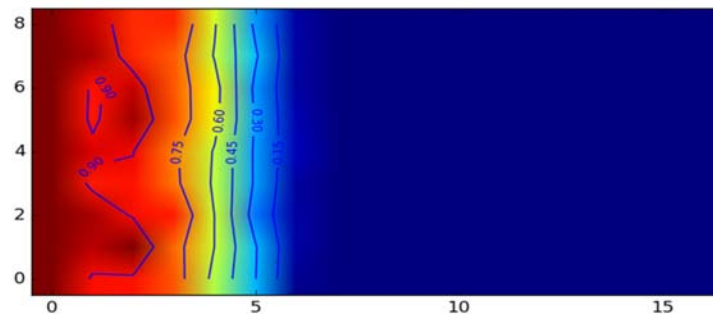
(b)



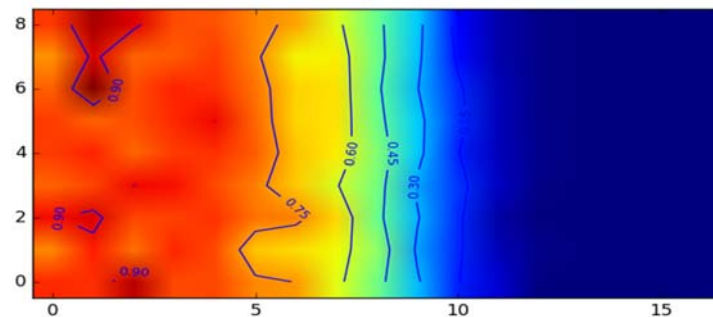
(c)

Figure 2.8 — Measured breakthrough curves fitted by ADE and CTRW-PT in heterogeneous media. Flow rates and measured dispersion coefficients are (a) 35 ml/min, 0.212 cm²/min, (b) 47 ml/min, 0.348 cm²/min, and (c) 70 ml/min, 0.898 cm²/min. Values of β are shown in each case.

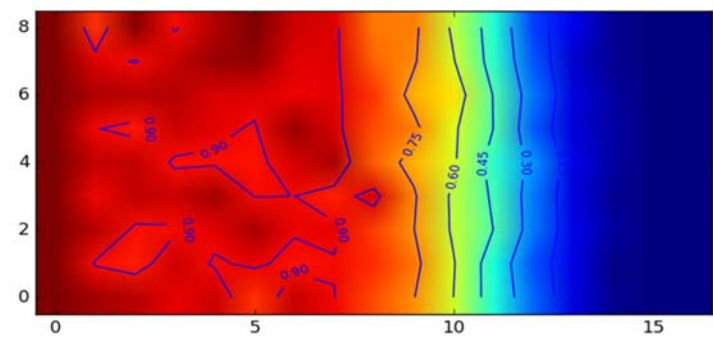
Figure 2.9 and 2.10 are concentration profiles in homogeneous and heterogeneous media at different time after injection, respectively. In homogeneous system, the fluid front advances like a piston where concentration gradient is uniform at any points at a certain distance along the flow direction (Figure 2.9). However, the competition of flow in heterogeneous system due to the difference of permeability between flow paths introduce the fingering-shape of fluid front (Figure 2.10). The particles tend to bypass the low-permeable sands and thus propagate in high-permeable sands next to the low-permeable ones. The red regions present the propagation of particles in high-permeable sands.



(a)



(b)



(c)

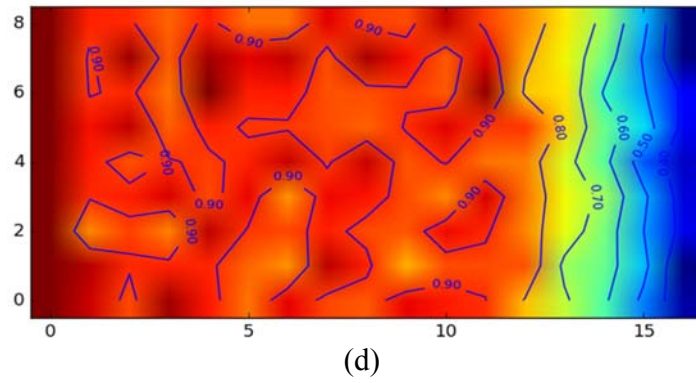
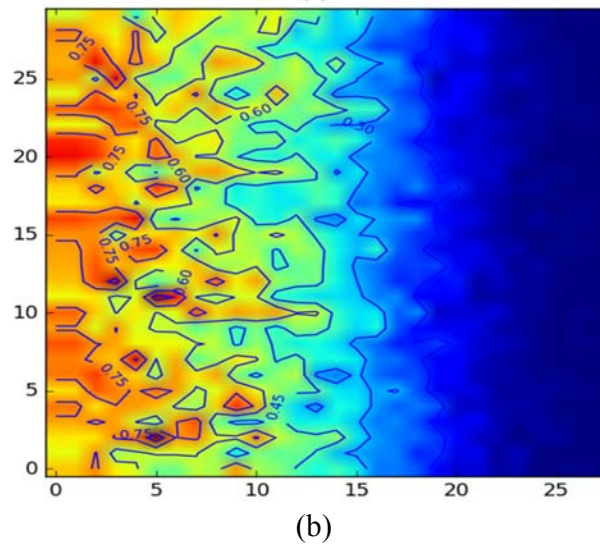
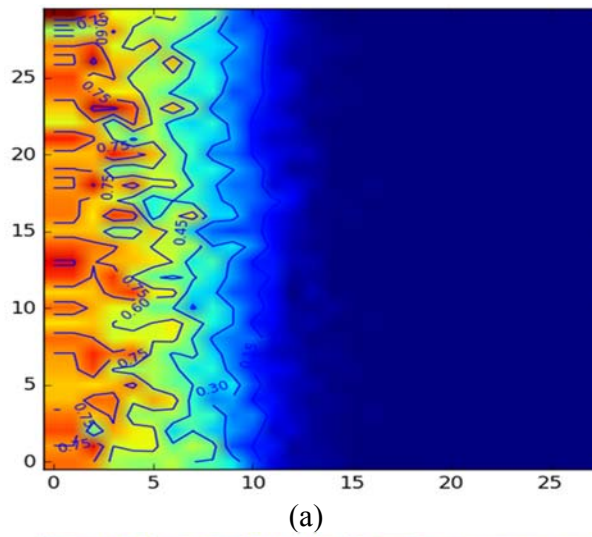
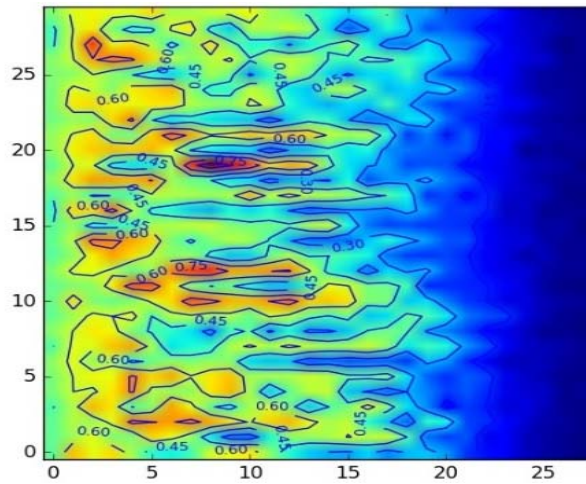
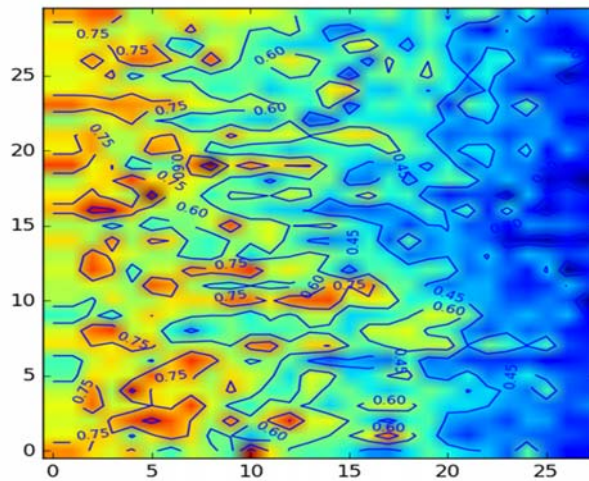


Figure 2.9 — Concentration profiles of the case with injection rate of 36 ml/min in homogeneous system at time of (a) 50, (b) 100, (c) 200 and (d) 300 minutes.





(c)



(d)

Figure 2.10 — Concentration profiles of the case with injection rate of 35 ml/min in heterogeneous system at time of (a) 50, (b) 200, (c) 400 and (d) 600 minutes.

2.4.3 Sensitivity Analysis

To investigate the effect of characteristic parameters β and t_2 on flow behaviors, several simulations are run with various β and t_2 to show the sensitivity of the two important parameters in CTRW-PT simulation. The flow condition used is the randomly heterogeneous case with injection rate of 35 ml/min.

Figure 2.11 shows simulated breakthrough curves with various β values and a constant t_2 of 5000 times of t_1 . As β decreases, the time of breakthrough delays and the curve deviates more to the right, meaning the flow appears more anomalous-like. Figure 2.12 show breakthrough results with various t_2 values and a constant β of 1.71. t_2 is the characteristic diffusion time which can be interpreted as the longest time for a particle to complete a transition distance. More dispersion and anomalous transport is observed with higher t_2 , which delays the time when the effluent dimensionless concentration becomes unity. Comparing two figures, it is found that β determines the time of breakthrough. The time of C/C_0 reaching 0.5 increases as β decreases, indicating that the ensemble transport is described by β . However, t_2 does not have a large influence on the time of breakthrough, but on the late time arrival. Greater t_2 brings more dispersion that leave the majority of plume behind the center. The delayed flush then is observed due to higher characteristic diffusion time t_2 .

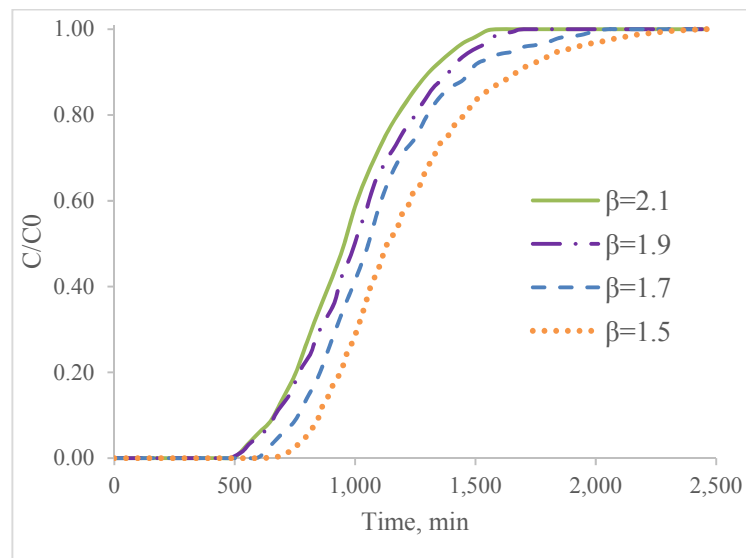


Figure 2.11 — Simulated breakthrough curves for tracer flow at injection rate of 36ml/min with various β and $t_2 = 5000 * t_1$.

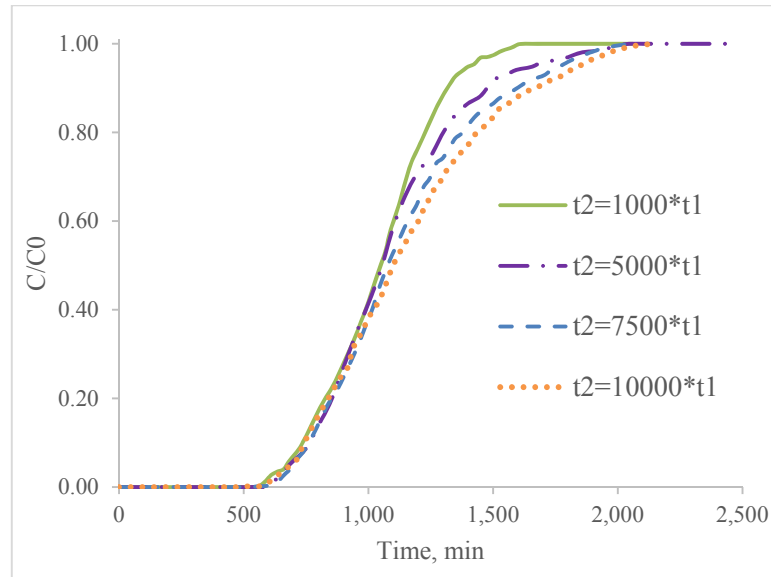


Figure 2.12 — Simulated breakthrough curves for tracer flow at injection rate of 36ml/min with various t_2 and $\beta = 1.71$.

2.5 Summary and Conclusions

The non-reactive tracer flow is simulated and fitted for the experimental results using CTRW-PT approach in this chapter. The joint space-time characteristic probability density function (pdf) is utilized as the core of this probabilistic approach. Two case studies of homogeneous and heterogeneous system are analyzed at different injection flow rate. β and t_2 values are compared in each case to describe the level of anomalous transport that how much it deviates from the normal transport. The sensitivity analysis shows that β is a more important parameter in CTRW-PT simulation. β describes the transport by controlling the range of random flow velocities of particles, which fundamentally represents the dispersion behavior. A smaller β stands for higher probability of longer transition time, smaller local flow velocity and more anomalous transport. It is indicated that the effect of heterogeneity and flow rate on the anomalous transport can be well described by β . The concentration profiles in 2-D rectangular

domain displays the completing of flow and significant figuring effect in heterogeneous media.

Chapter 3 Modeling Reactive Nanofluid Flow

3.1 Introduction

Reactive transport in porous media is always the interest in a wide range of fields such as environmental engineering, hydrogeological engineering and petroleum engineering (Singh 2014). The reaction between flowing fluid and porous media is a dynamic process that brings evolution of nature of porous media and further evolving the flow pattern and behavior. The examples of reaction include nanofluid adsorption and desorption, dissolution and precipitation of rock minerals due to reactive fluid flow, and the contamination of groundwater flow. Lopez-Chicano et al. (2001) studied drainage of calcium-rich surface water from springs. Berkowitz and Scher (1995) simulated precipitation, dissolution at core and field scales on several types of porous media by solving partial differential equations numerically incorporating a random walk process. Dentz et al. (2004) uses CTRW-PT approach to quantify bimolecular reactive transport, capturing the local fluctuations in concentrations at small scale and demonstrate the effects on the larger-scale behavior. A well-known application of reactive process is the matrix acidizing applied in oil and gas industry. There are many theoretical and practical researches on acidizing processes, with topics of modeling wormhole propagation, acid transport and rock dissolution and conductivity of fractures by acid fracturing (Buijse and Glasbergen 2005, Hill et al. 1995, Kalia 2008, Kamali and Pournik 2015, 2016).

The flow of reactive fluids in porous media is a competing process between transport and reaction. The process that involves advection, diffusion and reaction varies across spatial scales (Panga 2003). Advection is the transport of a substance by bulk fluid along the

direction of flow. The ability of the fluid transport is always measured by permeability of porous media. In natural porous media, the heterogeneity leads to various advective behaviors locally. Diffusion is always considered as fluid molecules moving from high-concentration region to low-concentration region. Both advection and diffusion occur over the entire domain of porous media. The local advection and diffusion are space-dependent effects as heterogeneous porous media displays spatial variability of physical properties. However, the reaction which originates at nanoscale can be considered to occur locally around the reaction front as a relatively faster process than advection or diffusion (Singh 2014). Therefore, the reaction can be treated as immediate process compare to transport. Therefore, reaction is modelled following by transport at the end of each time step. To avoid the flocculation of chemical alternation which would bring errors in simulating the change in fluid and reservoir properties, the time step must be appropriately set up (Edery et al. 2011).

In this study, the 2-D CTRW-PT approach shown in chapter 2 is utilized to simulate the nanoparticle fluid flow through Boise sandstone and Texas Cream limestone sand packs with the deposition of nanoparticles onto rock pore surface. Nanoparticles are small enough that they can pass through the reservoir rocks without plugging the pore throats. However, physicochemical interaction between the nanoparticles and the pore walls can adsorb nanoparticles on pore walls to bring significant retention of nanoparticles (Abdelfatah, Kang, Pournik, Shiau, Harwell, et al. 2017). However, the experimental data used to verify the validation of CTRW-PT approach are from injecting non-clustered small silica nanoparticles (with radius 5 to 10 nm) into sand packs (Caldelas 2010, Zhang 2012). Therefore, it is assumed that there is no mechanical plugging or screening occurred

during the process. The only reactive terms are deposition and release, which are combined as the net deposition in the simulation. The rate of deposition and release at different temperature, ionic strength, and pH are calculated based on DLVO theory that evaluates the interaction between nanoparticles the rock minerals. The calculated rates of deposition and release have been validated by solving ADRE numerically to well fit the experimental results (Abdelfatah, Kang, Pournik, Shiau, Harwell, et al. 2017). Here, the rates of deposition are used in CTRW-PT approach for modeling the deposition of nanoparticles during its transport through sand packs.

3.2 Mathematical Model and CTRW Formulations

Like tracer flow, the transport of nanofluid flow is also modelled by CTRW-PT approach. Same formulations are used to model nanofluid transport in heterogeneous porous media. Recall the joint space-time particle transition probability density function discussed in Section 2.2:

$$\psi(\vec{s}, t) = F(\vec{s})\psi(t) \quad (3.1)$$

$$pdf \text{ for space: } F(\vec{s})d\vec{s} = sp(s)ds\Omega(\phi)d\phi \quad (3.2)$$

$$p(s) = \lambda_s^2 \exp(-\lambda_s s) \quad (3.3)$$

$$\Omega(\phi) = \mathcal{N} [0, \sigma] \quad (3.4)$$

$$pdf \text{ of time: } \psi(t) = C \frac{\exp\left(-\frac{t}{t_2}\right)}{\left(1+\frac{t}{t_1}\right)^{1+\beta}}, \quad \text{Anomalous} \quad (3.5)$$

where,

$F(\vec{s})$ is the pdf of spatial increments.

$\psi(t)$ is the pdf of temporal increments.

$p(s)$ is the pdf of transition distance along the flow direction.

$\Omega(\phi)$ is the pdf of angular vector for transition distance.

$\psi(t)$ is the pdf of transition time which follows exponential distribution for normal transport and a combined exponential-TPL distribution for anomalous transport.

t_1 is the characteristic advection time.

t_2 is the cut-off time to normal transport, or characteristic diffusion time.

β is the power law exponent.

λ_s , λ_t and C are normalization coefficients.

3.3 Modeling reactive processes

The CTRW-PT approach models the transport of nanoparticles. Now the reaction between nanoparticle and rock pore surface is incorporated into CTRW-PT approach to simulate the reaction dynamics depending on the rate of deposition and release. In each time step, the simulation of transport is conducted first, followed by the simulation of reaction. It is worth mentioning that the conceptual ‘particles’ to track in the CTRW-PT simulation is not the physical nanoparticles. In Chapter 2, each particle for simulation is assigned a share of certain mole of NaCl. Here, each particle carries a certain mass of silica nanoparticles. Because the concentration of nanofluid is given in the unit of volumetric percentage, each particle is assigned a volume based on the flow rate and time step. As discussed in section 2.3, all particles are frozen at the end of each time step. At this moment, a stochastic process is conducted to determine the fate of particles, in other words, which particle is going to be deposited on rock pore surface and disappear from the flowing system. The reaction dynamics of nanoparticles as a function of net rate of deposition is expressed in equation 3.6:

$$\frac{\partial C_{dep}}{\partial t} = K_{dep} * C_{particle} \quad (3.6)$$

where,

C_{dep} is net concentration of particle deposited on rock surface

K_{dep} is net rate of deposition.

$C_{particle}$ is the concentration of particle in the block at the end of current time step.

A stochastic process is utilized in modeling the reaction dynamics. The simulation steps of reactive process of nanoparticle deposition are:

1. According to equation 3.1, the ratio of particle that will be deposited during current time step is $\frac{C_{dep}}{C_{particle}} = K_{dep} * dt$
2. Then the possibility of a particle to deposit at the end of each time step is defined as $K_{dep} * dt$, which is dimensionless.
3. For each particle, a random number between 0 and 1 following uniform distribution is generated;
4. A stochastic process is proceeded to determine whether a particle deposits or continues to flow: if the generated random number is greater than $K_{dep} * dt$, this particle is safe to stay in the system; otherwise, the particle loses its location in the x-y coordinate to disappear.
5. A mass balance check is conducted to ensure the summation of retention and effluent equal to the total injection.

3.4 Results and Discussions

3.4.1 CTRW-PT simulation results

Four sets of experimental results are fitted to evaluate the effect of injection rate and rate of deposition. Table 3.1 show the parameters used in the experiments and simulations. The permeability profile of the sand pack is assumed to normally distribute with a standard deviation of 50. Different standard deviations yield different level of heterogeneities. In this case, it is set to be small because the sand pack is prepared by the same meshed sand.

Table 3.1 — Parameters used in the experiments and simulations.

Nanoparticle type	Nexsil 20K Silica	3M Fluorescent Silica
rock	Texas Cream Limestone	Boise Sandstone
Nanoparticle radius	10	5
Reference and experiment number	(Caldelas 2010) #33 and # 45	(Zhang 2012) #102 and # 107
Injection rate, $\text{cm}^3 \cdot \text{min}^{-1}$	1	1 and 10
Low rate of deposition, $\text{m} \cdot \text{s}^{-1}$	$1.03 \cdot 10^{-8}$	$2.74 \cdot 10^{-4}$
High rate of deposition, $\text{m} \cdot \text{s}^{-1}$	$3.16 \cdot 10^{-3}$	$2.74 \cdot 10^{-4}$
Dispersion Coefficient, cm^2/s	0.025 and 0.075	0.018, 0.152
Domain length, cm	30	
Domain width, cm	5	
Domain height, cm	0.2	
Number of blocks	30x5	
Initial porosity	0.4	
Initial permeability, md	800	
Molecular diffusion Coefficient, cm^2/s	$4.37 \cdot 10^{-7}$	

Experiment #33 and #45 conducted by Caldelas (2010) are simulated and fitted. Experiment #33 has a low rate of deposition and experiment #45 has a much higher rate (Figure 3.1). The two simulated breakthrough curves have similar shape where the one with higher rate of deposition has an about 150 seconds delay. CTRW-PT simulation results show similar transport behavior of those two experiments because of the same porous media and flow pattern. The smaller estimated mean flow velocity causes the delay of the one with higher rate of deposition. A smaller β value demonstrate that the macroscopic transport behaves more anomalous (Berkowitz et al. 2000), which is due to the retention of nanoparticles. Figure 3.2 show the concentration profiles of the above two cases. Due to the deposition of nanoparticle, the peak of plume in high-rate-of-deposition case is way behind the one in low-rate-of-deposition case. The heterogeneity in porous media leads to concentration gradient in the porous media, especially for the high-rate-of-deposition case. The anomalous transport is more severe with a high rate of deposition. After 2 pore-volume injected (PVI) or 1100 minutes, the sand pack is flushed by nanofluid. Comparing Figure 3.2 (a) and (b) at 1100 minutes, there is more anomalous behavior shown by concentration gradients in high-rate-of-deposition case (b).

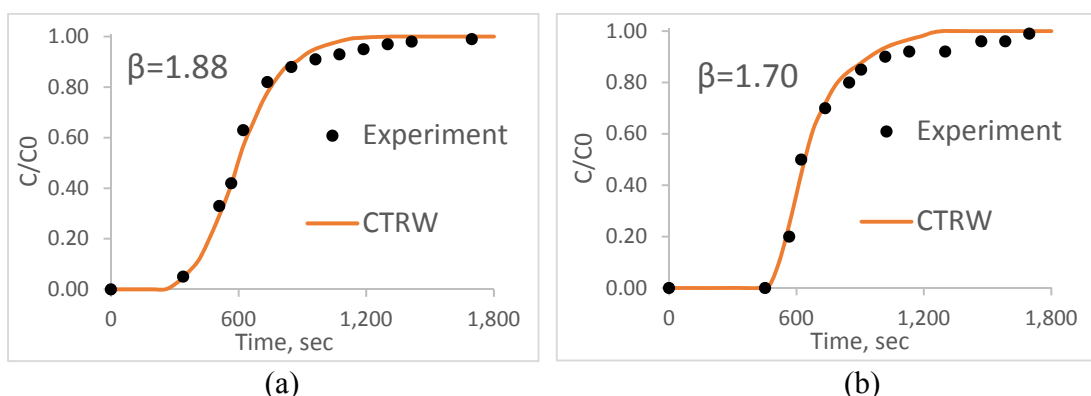


Figure 3.1— Fitted breakthrough curves for experiment a) low rate of deposition and b) high rate of deposition at the same injection rate of 1 ml/cm³.

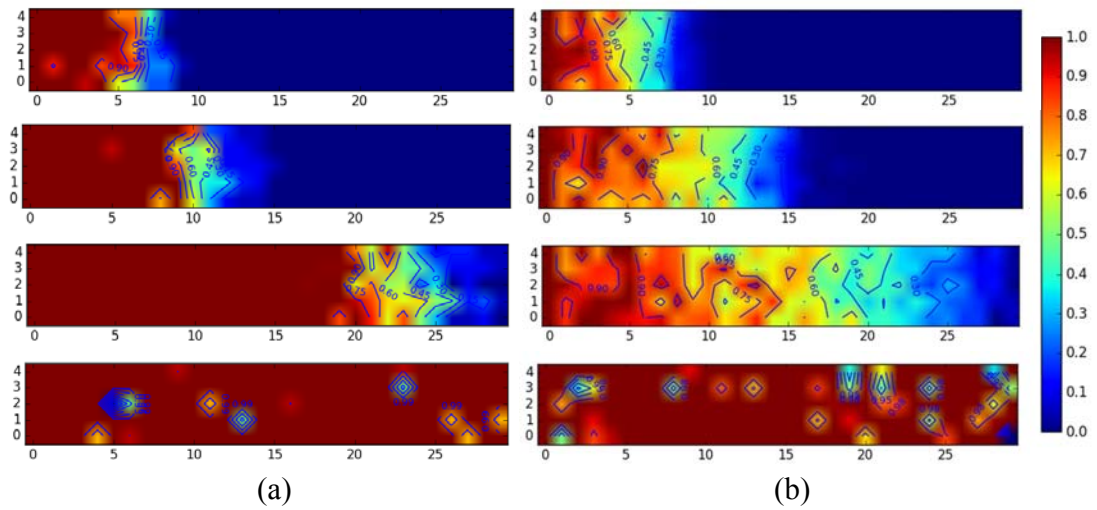


Figure 3.2 — Concentration profiles of simulation of (a) experiment #33 with low rate of deposition and (b) experiment #45 with high rate of deposition at 200, 300,400 and 1100 minutes from top to bottom.

Experiment #102 and #107 which both have a moderate rate of deposition conducted by (Zhang 2012) are simulated and fitted to learn the effect of injection rate. With a ten times of injection rate, simulation of experiment #102 gives a much smaller β than experiment #107. However, this value is not as small as the heterogeneous cause analyzed in chapter 2. Figure 3.3 show the fast breakthrough with high injection rate has a steeper shape than low injection rate, with a smaller β . There is more anomalous transport occurring at high injection rate. Figure 3.4 show the concentration profile of the equivalently converted 2-D domain from the 3-D cylindrical sand pack. The sand packs are prepared with the same types of rock grains and so the permeability is assumed to follow a normal distribution. The profiles show the level of anomalous transport is less than randomly heterogeneous case and greater than homogeneous case discussed in chapter 2. After two pore volumes have been injected and the sand pack is flushed, there are still anomalous transport occurring through the sand pack.

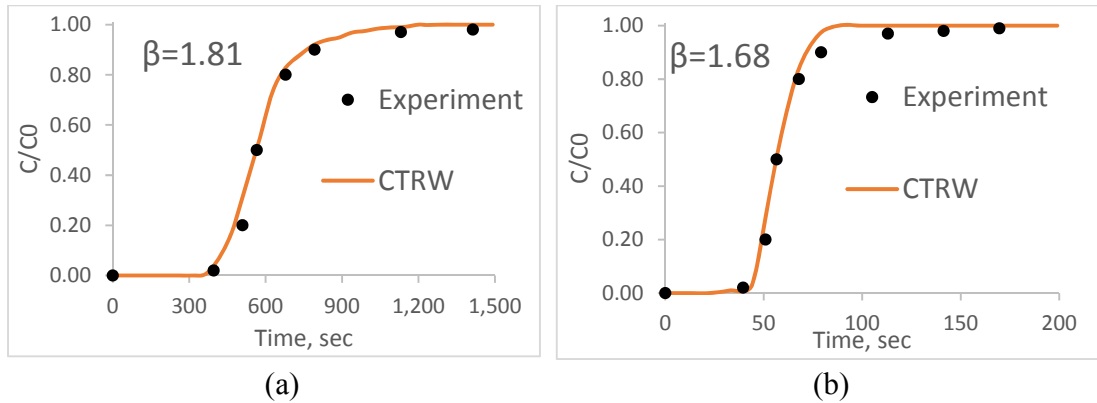


Figure 3.3 — Fitted breakthrough curves for experiment (a) low injection rate of 1 ml/cm³ (# 107) and (b) high injection rate of 10 ml/cm³ (# 102) with similar rate of deposition.

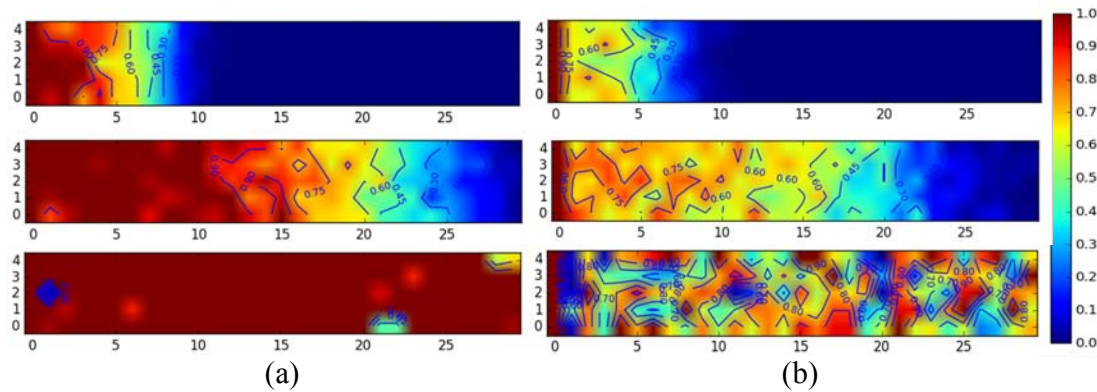


Figure 3.4 — Concentration profiles of simulation of (a) low injection rate of 1ml/cc (#107) and (b) high injection rate of 10 ml/cc (#102) at same PVI (Pore volume injected).

3.4.2 Sensitivity Analysis

To investigate the effect of characteristic parameters β and t_2 on reactive flow, several simulations are run with various β and t_2 to show the sensitivity of the two important parameters in CTRW-PT simulation. The flow and fluid condition used is experiment #45 which has an injection rate of 1 ml/min and a high rate of deposition.

Figure 3.5 shows simulated breakthrough curves with various β values and a constant t_2 of 2000 times of t_1 . β controls the shape of breakthrough curves from early-time

breakthrough to late-time flush. As β decreases, the breakthrough delays due to longer transition time increments and thus smaller random transition velocities. Figure 3.6 show breakthrough results with various t_2 values and a constant β of 1.7. Without delaying early-time breakthrough, greater t_2 leads to more dispersion which delays the late-time flush. Comparing to the tracer simulation, varying β and t_2 with same amount for reactive flow shows more deviation from results of the reference case. The deposition of nanoparticles which disappear form flow system contributes to the ensemble anomalous-like flow behavior.

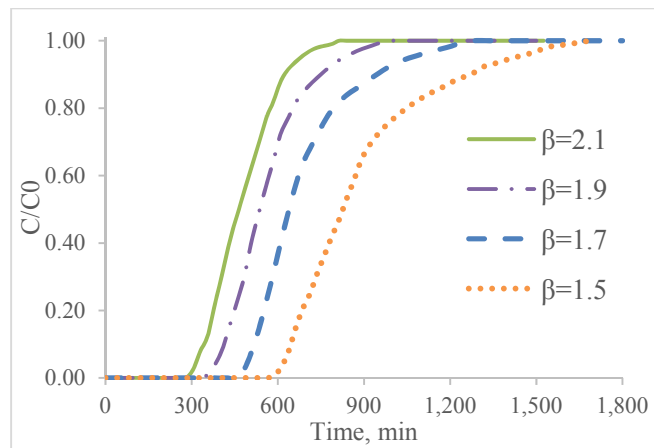


Figure 3.5 — Simulated breakthrough curves for nanofluid flow experiment #45 at injection rate of 1ml/min and high rate of deposition with constant $t_2 = 5000 * t_1$.

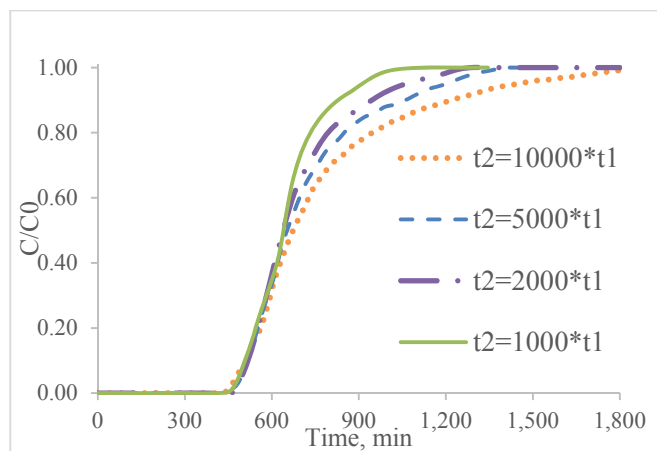


Figure 3.6 — Simulated breakthrough curves for tracer flow experiment #45 at injection rate of 1ml/min and high rate of deposition with constant $\beta = 1.7$.

3.5 Summary and Conclusions

The reactive nanofluid flow is simulated and fitted for the experimental results using CTRW-PT approach in this chapter. The transport of nanoparticle is simulated Using the same procedures of CTRW-PT approach. The modeling of reaction between nanoparticle and rock pore surface is incorporated into the transport modeling. A stochastic process is used to determine the fate of nanoparticle and the validation is check by mass balance of deposition and recovered nanoparticle equaling to the total nanoparticle injected. The effect of different conditions like rate of deposition and injection rate are studied. It is concluded that higher rate of deposition and higher flow rate make the fluid flow more anomalous. In addition, β values are compared in each case and it is found that the heterogeneity has more influence on β . The sensitivity analysis shows reactive flow behaves more anomalous than non-reactive flow with the same β due to the loss of solute. The value of β , describing level of anomalous transport, is more dependent on the nature of porous media. It is hypothesized that not only the heterogeneity, but also the length scale which may bring scale-dependent heterogeneity, has effect on anomalous behavior. This hypothesis will be studied and discussed in Chapter 4.

Chapter 4 Scale Up Tracer and Nanofluid Flow

4.1 Introduction

Due to the gap between well understanding and practices of fluid flow in laboratories and deviated observations of field responses, an appropriate and efficient method of scaling up is always interesting area of research. Mostofizadeh and Economides (1994) proposed a simple volumetric method to directly scale up laboratory results to field scale. (Bitarafhaghighi 2015) scaled up acidizing process using ADRE to simulate the acid transport and reaction and statistical approach to treat the reservoir properties. Singh (2014) scale up the CO₂ injection using particle tracking approach to simulate transport and scaling up reaction parameters spatially. In petroleum engineering, the predictions of treatments always depend on information obtained from the small-scale laboratory experiments, such as core flooding tests. However, discrepancies of results are always observed between different scales. The recovery factor during the injection of reactive fluids decreases from core flooding, pilot tests to field processes (Singh 2014). It shows that the simple volumetric method of scaling-up may not yield accurate results, especially when the porous media is heterogeneous (Li et al. 1996). In real world, the particles move through pore spaces along continuous paths, the CTRW assigns temporal and spatial transition increments to particles is considered as a computational discretization of the pore-to-pore path and corresponding time spent on the path. Dentz et al. (2008) suggest that CTRW-PT approach is highly effective in quantifying bimolecular reactive transport with capture the large-scale behavior. Edery et al. (2011) simulated and scaled up

Dissolution and precipitation dynamics during dedolomitization using CTRW-PT approach. demonstrate pore-to-field-scale simulations for single-phase flow based on the same approach. They develop 2D to 3D lattice models with nodes denoting pores and only focus on time transition probability distribution. The approach of scale-up transport and reaction process based on small-scale information and the simulation results are presented in this chapter.

4.2 Scale-up approaches

4.2.1 Scale up reservoir properties

The permeability and porosity which may be changed by the reactive processes is the target reservoir properties to be scaled up. The change of nature of porous media may bring bias to the following transport and reaction processes. The simulations in section 3.4 show deposition of nanoparticles does not change porosity very much. The volumetric averaged method can be used to scale up porosity (Whitaker 2013). Recalling the objective of this research which is to predict flow behavior at large scale based on the flow response obtained at small scale, it is assumed that the information of permeability and porosity at small scale are accessible, which may come from mercury injection or CT scan. Then the objective becomes to represent large-scale heterogeneity based on small-scale data. Singh (2014) introduces a covariance model to scale up the reservoir properties. Because the small-scale geologic structures are embedded within the larger scale structures, it is assumed the characters of reservoir properties keep consistent across scales, for conventional reservoir rocks. Therefore, the properties in coarse grid blocks at small scale can be scaled up to large scale by downscaling the grid blocks (Figure 4.1).

The heterogeneity in finer grid blocks shows spatial variability at large scale with consistent covariance. In this model, the consistency of reservoir properties from small scale to large scale is described by matching the covariance of fine grid blocks, $Cov(i, i')$ to the covariance of their corresponding coarse grid blocks, $Cov(BI, BJ)$.

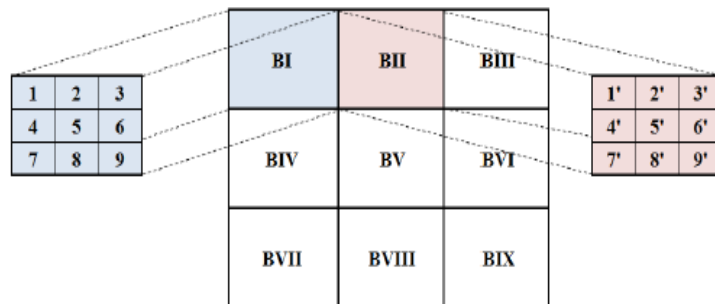


Figure 4.1 — Schematic of a reservoir property at two scales (Singh 2014).

As shown in Equation 4.1, the difference between covariance of coarse grid blocks (BI, BJ) and fine grid blocks (i, i') must be minimized to achieve the consistency across scales (Singh 2014):

$$\min\{Cov(BI, BJ) - Cov(i, i')\}^2 \quad (4.1)$$

The procedures of scale up and downscaling is explained using the sample shown in Figure 4.1. In the schematic, coarse grid blocks BI through BIX represent the measurements of a physical property of a 3cm x 3cm sample with 9 grid blocks. Before downscaling, it is expected that it would be scaled up to a 9cm x 9cm region with 81 grid blocks. During downscaling, the properties in blue and pink blocks have the same covariance as it of grid blocks BI and BII. After the downscaling, consistent features are maintained between small and large scales, which are 3cm x 3cm domain with 9 grid blocks and 9cm x 9cm domain with 81 grid blocks, respectively. Arithmetic and harmonic

averaging methods are applied to control the size and number of grid blocks if the downscaled grid is too fine.

4.2.2 *Scale up transport using CTRW-PT approach*

The proposed CTRW approach let us to select spatial and temporal discretizations, which provides a direct access to scale-up the transport process. As the domain with finer grid blocks which represents larger scale heterogeneity and length scales, the CTRW-PT model is run with the scale-up domain, keeping the parameters that best fits the experimental data unchanged. To maintain the character of the flow, the parameter β is not changed. This guarantees the flow has consistent behavior at large scale as it is at small scale. The injection rate is increased as the same times the domain volume increases, which can be simply calculated from new domain volume divided by previous domain volume. Solving Equation 2.9 with corrected injection rate and estimated D_ψ yields new t_1, t_2 for the flow at larger scale. The dispersion coefficient is assumed to be consistent to represent the same flow behavior in fine grid blocks at smaller scale. The estimated dispersion coefficient can be roughly estimated from the experiments with similar injection rate. It is interested that how length scale and scale-dependent heterogeneity change the final response of flow at large scale if the flow behavior at small scale has been captured.

4.3 Results and Discussions

4.3.1 Scale up tracer flow in homogeneous system

The tracer flow of homogeneous case at injection rate of 74 ml/min is chosen to scale up by 5 and 10 times, respectively. The domain at lab scale has a size of 86-cm long and 45-cm wide with grid blocks 17 x 9. To scale up 5 times the grid block becomes 85 x 45, representing a 4.3 m x 2.25 m domain. Scaling up 10 time yields grid block of 170 x 90 which representing 8.6 m x 4.5 m domain. The height of the domain does not change because the simulation is run in a 2-D model. The injection rates are increased 25 and 100 times to be consistent with the increasing in domain size. Figure 4.2 shows the breakthrough curves which the delay is observed at larger scale. However, the shapes of breakthrough curves are similar, which means the flow behavior at small scale is captured at large scale.

It is found that the flow characters of concentration profiles with fine grids are hard to tell due to the concentration flocculation brought by anomalous transport and uncertainties due to stochastic process. Instead, I simulated the flow by injecting from a single block at the inlet to better evaluate the dispersion visually at large scale. Figure 4.3 show the concentration map at lab scale and 5-time greater scale with time. More dispersion and observed at all time for the large-scale simulation. The amount of dispersion increases along the flow direction, which explains the delay tendency at larger scales observed in Figure 4.2.

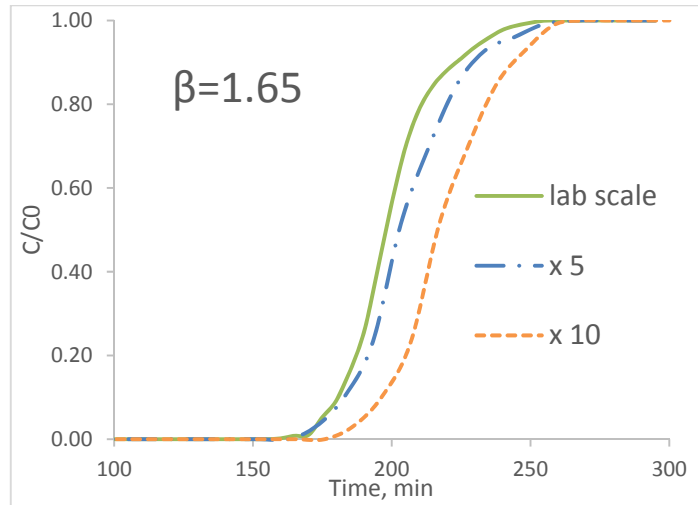


Figure 4.2 — Simulated breakthrough curves of tracer flow with injection rate of 74 ml/min, scaled up with 5 and 10 times.

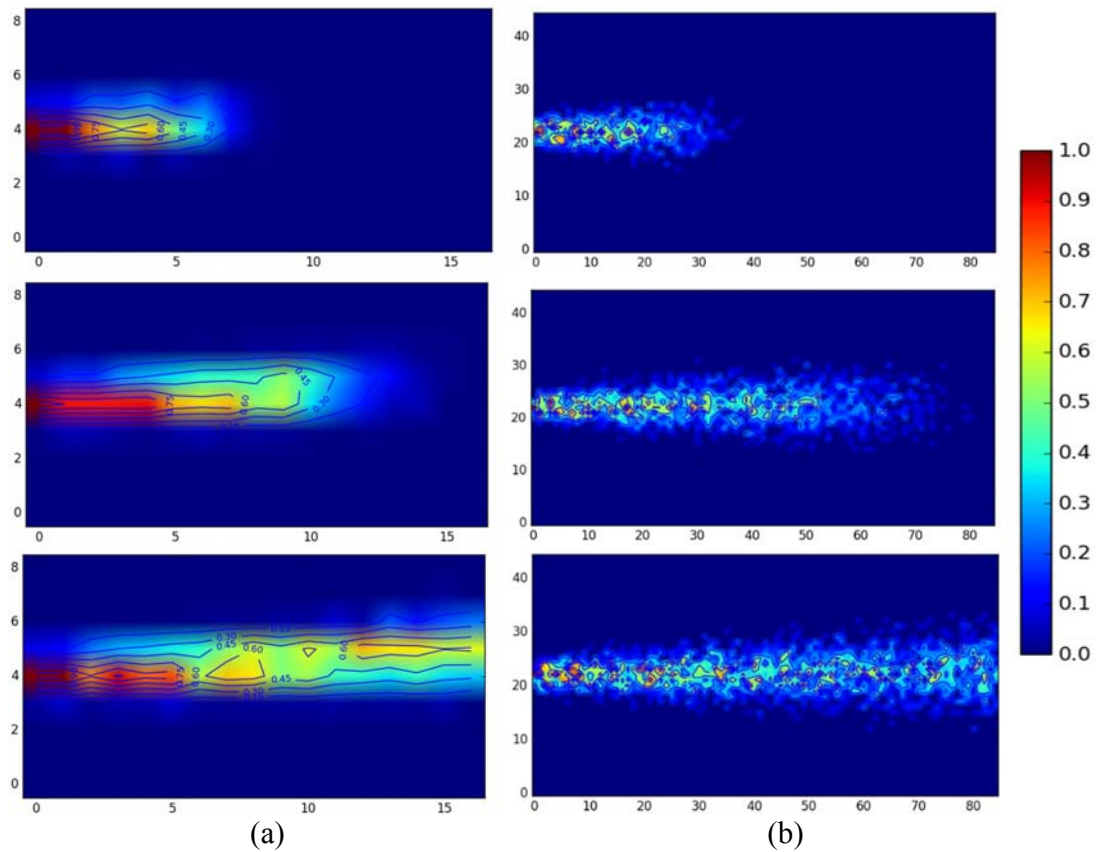


Figure 4.3 — Concentration maps of tracer flow injected through one block at lab scale (a) and scaled up with 5 times (b) at time of 50, 100 and 200 minutes from top to bottom.

4.3.2 Scale up nanofluid flow in heterogeneous system

The nanofluid flow of heterogeneous at injection rate of 74 ml/min is chosen to scale up by 2 and 4 times, respectively. The domain at lab scale has a size of 30-cm long and 5-cm wide with grid blocks 30 cm x 5 cm. To scale up 2 times the grid block becomes 60 cm x 10 cm, representing a 0.6 m x 0.1 m domain. Scaling up 4 times yields grid block of 120 x 20 which representing 1.2 m x 0.2 m domain. Figure 4.4 show the scaled-up permeability map by two and four times. Figure 4.5 show the simulated breakthrough curves from small to large scale. With only two and four times of scale-up compared to the homogeneous case which are five and ten times, the delay of breakthrough is more severe. The simulated case is experiment #45 by Caldelas (2010) with a high rate of deposition. Figure 4.6(a) shows the concentration map at lab scale. Unlike to straight breakthrough shown in Figure 4.3(a) in homogeneous system, the heterogeneity and high rate of nanoparticle deposition lead to the concentration gradient all over the media. Figure 4.6(b) shows the concentration gradient distributed with more transverse dispersion at large scale. The heterogeneity at larger scale increases the competition of fluid flow and thus delays the breakthrough.

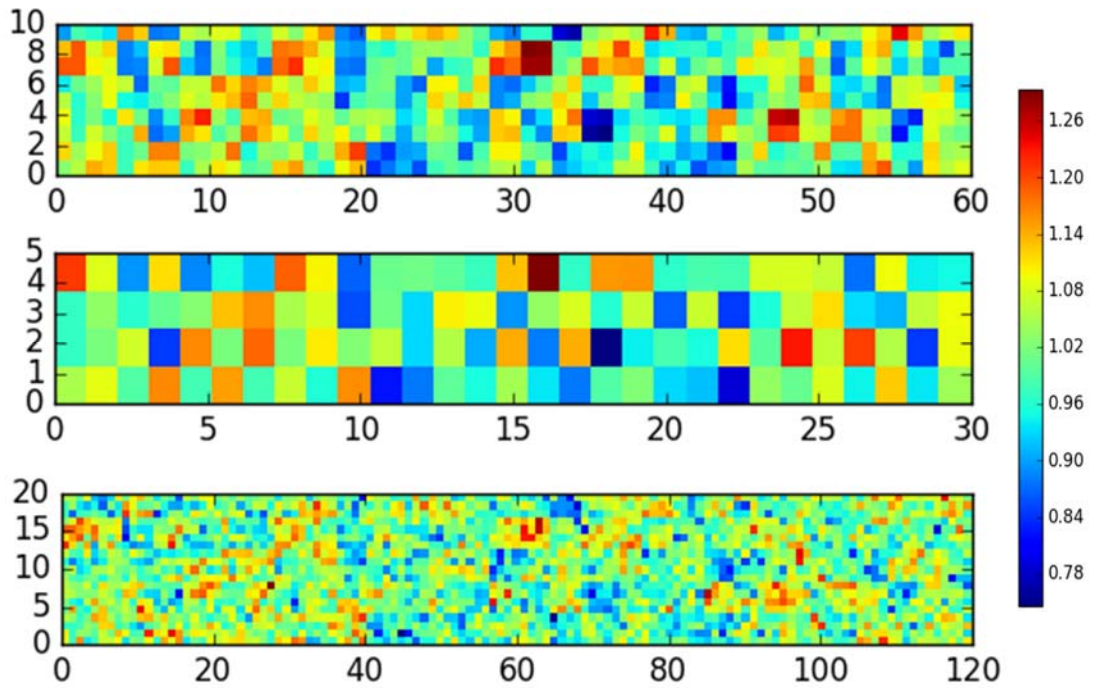


Figure 4.4 — Relative permeability map at different spatial scales (a) lab scale, (b) scaled up for two times and (c) scaled up for four times.

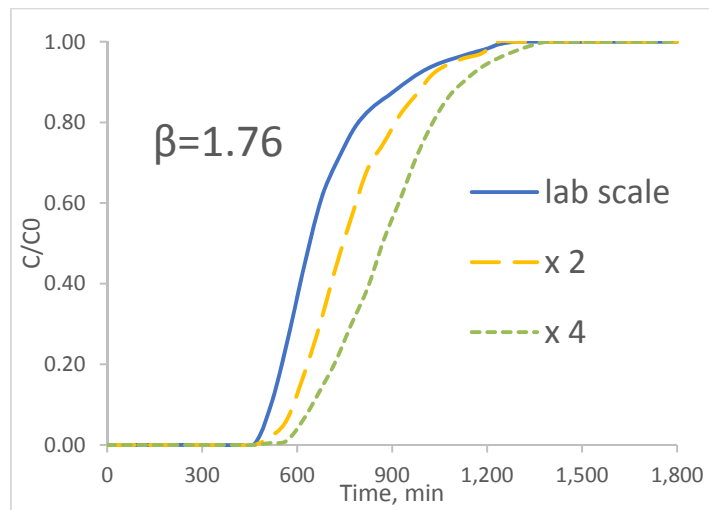
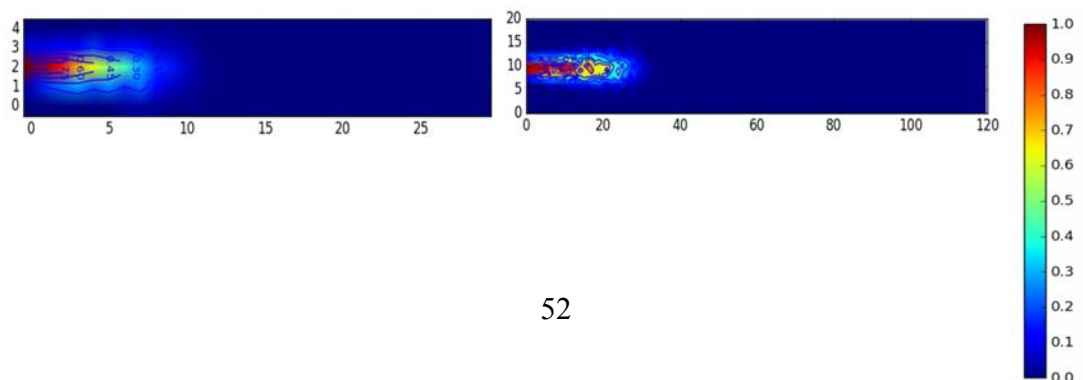


Figure 4.5 — Simulated breakthrough curves of nanofluid flow experiment#45 at injection rate of 1 ml/min and high rate of deposition, scaled up with 2 and 4 times.



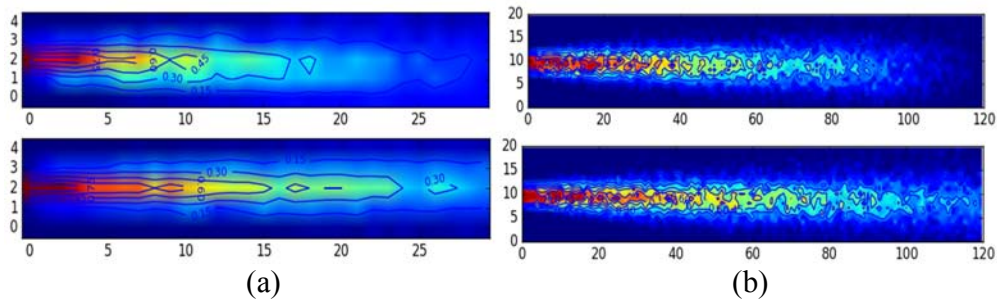


Figure 4.6 — Concentration profiles of simulation of nanofluid flow experiment #45 injected through one block (a) at lab scale and (b) scaled up with 4 times at 200, 500 and 1500 minutes.

4.3.3. Computational time of CTRW-PT and FDM approaches

Table 4.1 displays CPU time costed for simulating nanofluid flow with grid blocks 60 x 10 using CTRW-PT approach and solving ADRE by Finite Difference Method (FDM). The codes are run in Python 2.7.0. Comparing the two approaches, CTRW-PT saves more computational time than FDM. The results of CTRW-PT show that the computational time is more sensitive to number of particles tracking than size of grid blocks. It is due to the CTRW-PT model can be applied into a grid-free heterogeneous system if the concentration profile is not the objective, or into a grid-free homogeneous system with generation of the concentration profile. However, the memory needs to record large number of particle in each step will accumulate with time steps, resulting in more and more demand to calculate and store the spatial and temporal data for all particles. Large number of particles chosen to track in each time step decreases the uncertainty during the stochastic process, while it requires more computational resources. To choose an appropriate number of particles to track in each time step is critical to the quality of CTRW-PT simulation.

Table 4.1 — Recorded CPU time in seconds using CTRW-PT and Finite Difference Method in Python 2.7.0, with a grid size of 60 x 10.

Time Step	CTRW-PT		ADRE-FDM
	Inject 100 particle/time step	Inject 500 particle/time step	
1000	879	2252	3028
600	496	928	1214
300	175	386	576

4.4 Summary and Conclusions

A downscale modeling is applied to scale up the reservoir property. The permeability distributed in finer grids equivalently represents the scaled-up region with consistent covariance. Non-reactive tracer flow in homogeneous system is scaled up by 5 and 10 times. The dispersion and anomalous behavior is shown in the simulation case of injecting through a single centered grid block at inlet. More dispersion at larger scale is observed in the concentration profile when the parameters of CTRW-PT model are not changed. The reactive nanofluid flow in normally distributed permeability field is scaled up by 2 and 4 times. Comparing to the flow in homogeneous system, the heterogeneity at greater spatial scale leads to more delay of breakthrough, and more anomalous transport. Simulations between two simulation approaches in various conditions are run to compare the efficiency of CTRW-PT approach over solving ADRE by FDM. The CTRW-PT is more computationally effective than ADRE, especially in the scale-up cases. The computation efficiency of is more sensitive on number of particles tracked than the number of grid blocks because the particle tracking method can be applied in a grid-free system. Time step is always critical to the computation time for both CTRW-PT approach and ADRE-FDM.

Chapter 5 Conclusions and Future Work

5.1 Conclusions

The objective of this research is to scale up reactive flow to larger scale and predict the response based on the small-scale information. It is achieved by employing the CTRW-PT approach. Non-reactive tracer and reactive nanoparticle fluid flow have been simulated and matched to validate the model at laboratory scale. In several case studies, experiment results are fitted and CTRW approach shows the ability to capture anomalous behavior of late breakthrough which convectional ADRE does not achieved. The particle tracking approach is applied so that the flow front and shape are visible with time. The

CTRW framework incorporating PT method give rise to the realization of simulate fluid flow at various scales. A model is proposed to simply scale up reservoir permeability so that small-scale information can represent large scale region. Assuming the microscopic fluid transport and reaction behaves similar at macroscopic scale, CTRW-PT is used to scale up the fluid flow. The simulation results investigate the effect of flow rate, scale-dependent heterogeneity, chemical alternation and length scale on the behavior of fluid flow:

1. Spatial-dependent heterogeneity at large scale introduces more anomalous transport which delays the breakthrough of fluid. The delay can be estimated by two appropriate parameter β and characteristic diffusion time t_2 at small scale, in which the former parameter is more important in CTRW-PT simulation.
2. More heterogeneous system leads to more anomalous transport, which is well captured by smaller β and greater t_2 in CTRW-PT approach.
3. High flow rate brings higher dispersion and anomalous transport. However, the breakthrough will not delay much if the system is homogeneous.
4. The deposition of nanoparticle results in significant concentration gradient and late breakthrough, which are always evaluated by a small β as an ensemble.

The transport processes in reservoirs associated with chemical reactions are contributed by the fluid movement and reaction in terms of space and time in addition to geological heterogeneity. Coupled physical transport and chemical reaction processes have been described and simulated by the probabilistic approach of CTRW-PT. The transport of fluid is contributed by the superposition of spatial and temporal transitions, which are

chosen from the characteristic probability density function of CTRW during a stochastic process. The characteristic pdf lies the basis of the modeling by successfully represent the ensemble average of flow behavior in porous media. The advantages of this approach include:

1. It can better capture the anomalous behavior than solving ADRE numerically, especially in heterogeneous porous media.
2. It is an efficient approach to scale up the flow to larger scale based on the information obtained in laboratory.
3. It is more computationally efficient than solving convectional ADRE using Finite Difference Method or other similar numerical methods.
4. It can model reactive process which incorporates the transport process explicitly.
5. It used stochastic process in controlling the motion of fluid flow, which is more flexible in explaining unexpected results.

5.2 Plans for future work

A new model will be developed base on the CTRW-PT approach to simulate and model carbonate matrix acidizing. The large change on flow pattern and porous media and brought by acid reaction and rock dissolution is the major challenge which needs to be treated properly.

References

1. Abdelfatah, E., Kang, K., Pournik, M. et al. 2017. Study of Nanoparticle Retention in Porous Media-A Perfect Sink Model. Presented at the EAGE 19th European Symposium on Improved Oil Recovery, Stavanger, Norway, April 24-27. <https://doi.org/10.3997/2214-4609.201700233>
2. Abdelfatah, E., Pournik, M., Shiau, B. J. B. et al. 2017a. Mathematical Modeling and Simulation of Formation Damage Associated with Nanoparticles Transport in Porous Media. Presented at the SPE Latin America and Caribbean Mature Fields Symposium, Salvador, Bahia, Brazil, March 15-16. <https://doi.org/10.2118/184894-MS>.
3. Abdelfatah, E., Pournik, M., Shiau, B. J. B. et al. 2017b. Mathematical modeling and simulation of nanoparticles transport in heterogeneous porous media. *Journal of Natural Gas Science and Engineering* 40: 1-16.
4. Abdelfatah, E. R., Kang, K., Pournik, M. et al. 2017. Study of Nanoparticle Adsorption and Release in Porous Media Based on the DLVO Theory. Presented at the SPE Latin America and Caribbean Petroleum Engineering Conference, Buenos Aires, Argentina, May 17-19. <https://doi.org/10.2118/185484-MS>.
5. Abdelfatah, E. R., Soliman, M. M., Khattab, H. M. 2014. Improving Heavy Oil Recovery by Nanofluid Injection, The factors Affecting and Mathematical Modelling. *Journal of Petroleum and Mining Engineering* 17: 88-89.
6. Berkowitz, B., Adler, P. 2015. Dispersive transport across interfaces. Presented at the EGU General Assembly Conference Abstracts.
7. Berkowitz, B., Cortis, A., Dentz, M. et al. 2006. Modeling non - Fickian transport in geological formations as a continuous time random walk. *Reviews of Geophysics* 44 (2).
8. Berkowitz, B., Scher, H. 1995. On characterization of anomalous dispersion in porous and fractured media. *Water Resources Research* 31 (6): 1461-1466.

9. Berkowitz, B., Scher, H. 1998. Theory of anomalous chemical transport in random fracture networks. *Physical Review E* 57 (5): 5858-5869. <https://link.aps.org/doi/10.1103/PhysRevE.57.5858>.
10. Berkowitz, B., Scher, H., Silliman, S. E. 2000. Anomalous transport in laboratory - scale, heterogeneous porous media. *Water Resources Research* 36 (1): 149-158.
11. Bitarafhaghghi, V. 2015. Upscaling of the acidizing process in heterogeneous porous media. Master Thesis, West Virginia University, Morgantown, West Virginia.
12. Boggs, J. M., Young, S. C., Beard, L. M. et al. 1992. Field study of dispersion in a heterogeneous aquifer: 1. Overview and site description. *Water Resources Research* 28 (12): 3281-3291.
13. Buijse, M. A., Glasbergen, G. A semi-empirical model to calculate wormhole growth in carbonate acidizing. Society of Petroleum Engineers.
14. Caldelas, F. M. 2010. Experimental parameter analysis of nanoparticle retention in porous media. Master Thesis, University of Texas at Austin, Texas.
15. Dentz, M., Cortis, A., Scher, H. et al. 2004. Time behavior of solute transport in heterogeneous media: transition from anomalous to normal transport. *Advances in Water Resources* 27 (2): 155-173.
16. Dentz, M., Scher, H., Holder, D. et al. 2008. Transport behavior of coupled continuous-time random walks. *Physical Review E* 78 (4): 041110.
17. Dongxiao, Z., Winter, C. L. 1999. Moment-Equation Approach to Single Phase Fluid Flow in Heterogeneous Reservoirs.
18. Durlafsky, L. J. 2003. Upscaling of Geocellular Models for Reservoir Flow Simulation: A Review of Recent Progress. Presented at the 7th International Forum on Reservoir Simulation, Baden-Baden, Germany.
19. Edery, Y., Scher, H., Berkowitz, B. 2010. Particle tracking model of bimolecular reactive transport in porous media. *Water Resources Research* 46 (7).

20. Edery, Y., Scher, H., Berkowitz, B. 2011. Dissolution and precipitation dynamics during dedolomitization. *Water Resources Research* 47 (8).
21. Elimelech, M., Gregory, J., Jia, X. et al. 1995. Chapter 3 - Surface interaction potentials. In *Particle Deposition & Aggregation*, 33-67. Woburn, Butterworth-Heinemann.
22. Hill, A., Zhu, D., Wang, Y. 1995. The effect of wormholing on the fluid loss coefficient in acid fracturing. *SPE Production & Facilities* 10 (04): 257-264.
23. Kalia, N. 2008. Modeling and analysis of reactive dissolution of carbonate rocks. PhD Dissertation, University of Houston, Houston, Texas.
24. Kamali, A., Pournik, M. Rough Surface Closure—A Closer Look at Fracture Closure and Conductivity Decline. *International Society for Rock Mechanics*.
25. Kamali, A., Pournik, M. 2016. Fracture closure and conductivity decline modeling—Application in unpropped and acid etched fractures. *Journal of Unconventional Oil and Gas Resources* 14: 44-55.
26. Kitanidis, P. K. 1994. Particle - tracking equations for the solution of the advection - dispersion equation with variable coefficients. *Water Resources Research* 30 (11): 3225-3227.
27. LaBolle, E. M., Quastel, J., Fogg, G. E. 1998. Diffusion theory for transport in porous media: Transition - probability densities of diffusion processes corresponding to advection - dispersion equations. *Water Resources Research* 34 (7): 1685-1693.
28. Lake, L. W., Srinivasan, S., John, A. 2005. Statistical Scale-up: Concepts and Application to Reservoir Flow Simulation. In *Geostatistics Banff 2004*, ed. Oy Leuangthong and Clayton V. Deutsch, 681-690. Dordrecht, Springer Netherlands.
29. Leung, J. 2009. Reservoir Modeling Accounting for Scale-up of Heterogeneity and Transport Processes. PhD Dissertation, The University of Texas at Austin, Austin, Texas.

30. Levy, M., Berkowitz, B. 2003. Measurement and analysis of non-Fickian dispersion in heterogeneous porous media. *Journal of contaminant hydrology* 64 (3): 203-226.
31. Li, D., Cullick, A. S., Lake, L. W. 1996. Scale-Up Of Reservoir Model Relative Permeability Using A Global Method.
32. Lopez-Chicano, M., Bouamama, M., Vallejos, A. et al. 2001. Factors which determine the hydrogeochemical behaviour of karstic springs. A case study from the Betic Cordilleras, Spain. *Applied Geochemistry* 16 (9): 1179-1192.
33. McCarthy, J. 1993. Continuous-time random walks on random media. *Journal of Physics A: Mathematical and General* 26 (11): 2495.
34. Montroll, E. W., Weiss, G. H. 1965. Random walks on lattices. II. *Journal of Mathematical Physics* 6 (2): 167-181.
35. Mostofizadeh, B., Economides, M. Optimum injection rate from radial acidizing experiments. Society of Petroleum Engineers.
36. Panga, M. K. R. 2003. Multiscale Transport and Reaction : Two Case Studies. PhD Dissertation, University of Houston, Houston, Texas.
37. Qi, D., Hesketh, T. 2005. An Analysis of Upscaling Techniques for Reservoir Simulation. *Petroleum Science and Technology* 23 (7-8): 827-842. <http://dx.doi.org/10.1081/LFT-200033132>.
38. Rhodes, M., Bijeljic, B., Blunt, M. J. 2009. A rigorous pore-to-field-scale simulation method for single-phase flow based on continuous-time random walks. *SPE Journal* 14 (01): 88-94.
39. Salazar, M. O., Villa Piamo, J. R. 2007. Permeability Upscaling Techniques for Reservoir Simulation. Presented at the, 2007/1/1/.
40. Shook, M., Li, D., Lake, L. W. 1992. Scaling immiscible flow through permeable media by inspectional analysis (in English). <http://www.osti.gov/scitech/servlets/purl/6928846>.
41. Silliman, S., Simpson, E. 1987. Laboratory evidence of the scale effect in dispersion of solutes in porous media. *Water Resources Research* 23 (8): 1667-1673.

42. Singh, H. 2014. Scale-up of Reactive Processes in Heterogeneous Media. PhD Dissertation, The University of Texas at Austin, Austin, Texas.
43. Trefalt, G., Behrens, S. H., Borkovec, M. 2016. Charge Regulation in the Electrical Double Layer: Ion Adsorption and Surface Interactions. *Langmuir* 32 (2): 380-400. <http://dx.doi.org/10.1021/acs.langmuir.5b03611>.
44. Vlahos, L., Isliker, H., Kominis, Y. et al. 2008. Normal and anomalous diffusion: A tutorial. arXiv preprint arXiv:0805.0419.
45. Whitaker, S. 2013. The method of volume averaging, Vol. 13, Springer Science & Business Media (Reprint).
46. Zhang, T. 2012. Modeling of nanoparticle transport in porous media. PhD Dissertation, University of Texas at Austin, Austin, Texas.